DEMOCRATIC AND POPULAR REPUBLIC OF ALGERIA
MINISTRY OF HIGH EDUCATION AND SCIENTIFIC RESEARCH
UNIVERSITY OF MOHAMED BOUDIAF - M'SILA

FACULTY OF SCIENCES
DEPARTMENT OF PHYSICS

N° : PH/MAT/08/2024

DOMAINE: SCIENCE OF MATTER
FIELD : PHYSICS
OPTION : MATERIALS PHYSICS

Thesis Submitted for Obtaining
Diploma of Academic Master

By:

Seghiour Mohamed

Benarbia Abdelkrim

Entitled

Ab initio exploration of pressure effect on Structural parameters, electronic structure and magnetic properties of some perovskite compounds

Defended on 06/06/2024 in front of a jury composed of:

Djamel Allali	**University of Msila**	**Chairman**
Saber Saad Essaoud	**University of Msila**	**Supervisor**
Mohammed Elamin Ketfi	**University of Msila**	**Examiner**

Academic Year: 2023/2024

شكـر و تقديــر

مصداقا لقوله تعالى " ولئن شكرتم لأزيدنكم " فالشكر لله أولا و لرسوله الكريم علية افضل الصلاة و أزكى التسليم.

كما نتوجه بأخلص عبارات الشكر و التقدير الى استاذنا و مشرفنا على هذا العمل الاستاذ الفاضل **" صابر ساعد السعود "** على اشرافه ، دعمه و توجيهه المستمر و نصائحه القيمة خلال مراحل انجاز المذكرة، لك منا جزيل الشكر و العرفان.

و نشكر الاستاذ الفاضل **" جمال علالي"** على ترأسه اللجنة.

و نشكر ايضا الأستاذ الفاضل **" محمد الأمين كتفي"** على قبوله مناقشة هذه المذكرة.

الإهـــداء

الحمد لله الذي تتم بنعمته الصالحات، الحمد لله حمدا كثيرا مباركا فيه و الصلاة والسلام على أشرف سيد الخلق نبينا و شفيعنا محمد عليه أفضل الصلاة و أزكى التسليم,

إلى من لا يضاهيهما أحد في الكون، إلى من أمرنا الله ببرّهما،الى من سعينا دوما لإرضائهما، إلى من بذلا الكثير، وقدّما ما لا يمكن أن يردّ، إليكما تلك الكلمات الوالدان الغاليان، نهدي لكما هذا البحث؛ فقد كنتما خير داعم لنا طوال مسيرتنا الدراسية.

إلى الزوجتان اللتان جعلتا كلّ شيء ممكنًا بصبرهما ودعمهما.إلى المرأة ، شكرًأ على توفيركما لنا الظروف اللازمة لإكمال الدراسة نهديِ لكما هذا البحث.

الى أستاذنا "صابر ساعد السعود " الخلوق البشوش الذي لا تغادر الابتسامة وجهه في كل الظروف، نتمنى له دوام الصحة و العافية.

الى جميع الزملاء والأصدقاء.

"

Summary

List of tables

List of shapes

INTRODUCTION

Introduction

Solid materials have increasingly entered the manufacturing realm across various fields, including alternative renewable energies, where they are utilized in photovoltaic systems and thermoelectric generators. Among these solid materials are compounds known as perovskites, which follow the general formula (ABX_3). Their discovery in the mountains of Russia in 1993 marked a turning point in this field, as these materials are characterized by high stability and their ability to absorb light and heat, forming stable compounds suitable for various applications. Examples include $CsVO_3$ [1–3], $KMgF_3$, $AgMgF_3$[4], $BaNaCl_3$, $SrFeO_3$, and $SrVO_3$, which help overcome experimental obstacles such as time, cost, and various other factors. Software like Wien2K and Density Functional Theory (DFT) have been relied upon for such studies.

The compounds $CoAgF_3$ and $FeAgF_3$ were selected for their structural, magnetic, and electronic properties to determine their optimal utility. The study revealed that these compounds possess magnetic properties and have a simple cubic crystal structure with conductivity. The memorandum was organized as follows:

The first chapter provides a theoretical overview of studying any crystalline system based on Density Functional Theory (DFT) [5–10] , Hartree-Fock (HF) approximation, as well as the GGA and mBJ approximations to solve the Schrödinger equation.

The second chapter applies the concepts discussed in the first chapter using the WIEN2K program to calculate the structural properties, employing the GGA approximation for compounds $CoAgF_3$ and $FeAgF_3$. This includes parameters such as lattice constant (a), bulk modulus (B), and a study of their magnetic and electronic behavior.

References

[1] G A Kourouklis, A Jayaraman, G P Espinosa, and A S Cooper *J. Raman Spectrosc.* **22** 57 (1991).

[2] A V Ishchenko, K V Ivanovskikh, I A Weinstein, R F Samigullina, and V V Platonov *Radiat. Meas.* **124** 48 (2019).

[3] S Sâad Essaoud, A Bouhemadou, S Maabed, S Bin-Omran, and R Khenata *Philos. Mag.* 1 (2022).

[4] S S Essaoud, S M Al Azar, A A Mousa, and R S Masharfe *Phys. Scr.* **98** 035820 (2023).

[5] A Görling *Phys. Rev. A* **59** 3359 (1999).

[6] P Hohenberg and W Kohn *Phys. Rev.* **136** B864 (1964).

[7] Á Nagy *Phys. Rep.* **298** 1 (1998).

[8] B T Sutcliffe *Fundam. Electron Density Density Matrix Density Funct. Theory At. Mol. Solid State* 3 (2003).

[9] R G Parr *Horiz. Quantum Chem.* 5 (1980).

[10] T A Wesołowski *Chall. Adv. Comput. Chem. Phys.* 153 n.d.

the chapter1:

DENSITY FUNCTIONAL THEORY - AN OVERVIEW

CHAPTER 1:

DENSITY FUNCTIONAL THEORY - AN OVERVIEW

Table of Contents

1- The Schrödinger Equation

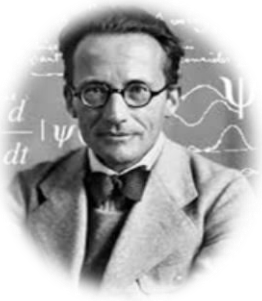

Within the context of quantum theory, scientist Erwin Schrödinger proposed a partial differential equation in 1926 that is now known as the Schrödinger equation [1–3]. By solving this equation, one can use the wave function—which contains all the information about the system under study—to explain the immediate quantum state of a system [1–3]. The following expression can be found in the Schrödinger equation:

$$H\Psi(\vec{R}_I, \vec{r}_i) = E\Psi(\vec{R}_I, \vec{r}_i) \text{.....(1)}$$

In this equuation, the two vectors $\vec{R}_I$and $\vec{r}_i$are the coordinates of the nucleus (I) and of the electron (i).

H: Hamiltonian operator related to the sum of the kinetic energy and the potential energy of the system.

E: eigenvalue Energy of the system.

Ψ: wave function which depends on the coordinates of electrons and nuclei.

The Hamiltonian system (made up of nuclei and electrons) consists the kinetic energy of electrons and nuclei, as well as the potential energies (electron-electron, electron-nucleus, and nucleus-nucleus), the expression for the total Hamiltonian effect of the system is givenas follows :

$$H = T_e + T_N + V_{ee} + V_{e-N} + V_{N-N} \text{..... (1.1)}$$

$T_e = -\sum_i \frac{\hbar^2}{2m_i} \vec{\nabla}_i^2$ →Electronic kinetic energy (m_i the mass of electron i.....(1.1.1)

$T_n = -\sum_I \frac{\hbar^2}{2m_I} \vec{\nabla}_I^2$ →Nuclei kinetic energy (m_I the mass of the nucleus I.....(1.1.2)

$V_{N-N} = \sum_{I \neq J} \frac{Z_I Z_J e^2}{|R_I - R_J|}$ →The interaction part between the nuclei.....(1.1.3)

$V_{e-N} = \sum_{I,j} \frac{Z_I e^2}{|R_I - r_j|}$ →The nuclei-electrons interaction part.....(1.1.4)

$V_{e-e} = \sum_{i \neq j} \frac{e^2}{|r_i - r_j|}$ →The interaction part between the electrons.....(1.1.5)

$|R_\alpha - R_\beta|$ → The distance between the two nuclei α and β (1.1.6)

$|r_i - R_\alpha|$ → The distance between the nucleus α and the electron i .....(1.1.7)

$|r_i - r_j|$ → The distance between the two electrons i and j.....(1.1.8)

In practical terms, solving the Schrödinger equation and achieving an exact solution poses considerable challenges, particularly when dealing with systems comprising numerous electrons and nuclei in dynamic interaction. Consequently, the necessity arises to employ simplifications and approximations to obtain an approximate solution that closely resembles the actual solution. Below are some of the most notable techniques and simplifications used to tackle this equation:

2- Born-Oppenheimer Approximation

The Born-Oppenheimer approximation [4], developed in 1927 by physicists Max Born and Robert Oppenheimer, made it possible to separate the motion of nuclei from the motion of electrons. Despite its movement, the nucleus remains very close to its equilibrium forthe electrons, which are very fast, and thus the kinetic energy of the nucleus can beneglected with respect to the kinetic energy of the electrons, kinetic energy and consider the nucleus-nucleus interaction energy as a constant quantity (V_{nn} = Constant).

According to the Born-Oppenheimer approximation we can rewrite the total wave function of the system $\Psi\left(\vec{R}_I^{\,0}, \vec{r}_i\right)$in the form of a product of an electronic function $\Psi_e\left(\vec{R}_I^{\,0}, \vec{r}_i\right)$and a nuclear function $\Psi_n\left(\vec{R}_I^{\,0}\right)$, thus, we can separate the motion of nuclei from that of electrons. Then the wave function is written:

$$\Psi\left(\vec{R}_I^{\,0}, \vec{r}_i\right) = \Psi_n\left(\vec{R}_I^{\,0}\right)\Psi_e\left(\vec{R}_I^{\,0}, \vec{r}_i\right) \text{ .....(2)}$$

Despite applying this simplification to the Schrödinger equation, the equation remains difficult to solve and cannot be solved using current mathematical methods due to the extremely complicated electron-electron interaction, So we used additional approximations.

3- Hartree and Hartree-Fock Approximations (HF)

To improve and address the drawbacks of the Hartree approximation, the Hartree-Fock approximation was put out. The independent particle approximation, which Hartree suggested in 1928[5,6], treats all electrons as identical particles that travel independently of one another without interacting with other particles. The interactions that take place between electrons are Columbian repulsion interactions, with exchange and correlation terms ignored, because Hartree sees the electrons as charged particles in this approximation and ignores the spin state. Furthermore, because it disregards the Pauli exclusion principle, the wave function is not symmetric [2,3].

Although the Hartree approximation does not take in account the electron spin and the Pauli exclusion principle, it simplifies the Schrödinger equation from studying a large number of electrons to studying a single electron, so that the total Hamiltonian H of electrons is the sum of the Hamiltonians hi of each electron, while the total wave function of the electronic system represents by multiplication the individual wave functions of each electron [2,3]. Finally, the total energy of the electronic system equals the sum of the individual energies of all electrons. Using Hartree's approximation, the Hamiltonian equation for a single electron can be expressed as follows:

$$H = \sum_i h_i \ldots\ldots\ldots\ldots\ldots\ldots\ldots\ldots\ldots\ldots (3)$$

$$h_i = -\frac{\hbar^2}{2m_i}\Delta_i - \sum_I \frac{Z_I e^2}{\left|\vec{r_i} - \vec{R_I}^0\right|} + \frac{1}{2}\sum_j \frac{e^2}{\left|\vec{r_i} - \vec{r_j}\right|} \ldots\ldots\ldots\ldots (3.1)$$

$$\Psi_e = \prod_i \Psi_i \ldots\ldots\ldots\ldots (3.2)$$

$$E_e = \sum_i \varepsilon_i \quad \ldots\ldots\ldots\ldots\ldots\ldots\ldots\ldots (3.4)$$

In 1930, Fock [7] modified Hartree's model by substituting the wave functions of the electron with a Slater determinant[8], allowing him to accommodate for the exchange effect that Hartree neglected. In this way, the interaction between electrons takes into account both the Coulomb interaction and the exchange effect, and thus the previous functions have been replaced by anti-symmetric functions, and therefore, Fock introduced the term spin in its dealing with electronic interactions and replaced the wave function of the electronic system by a Slater determinant and this determinant is expressed by the formula:

$$\Psi_{HF}(\vec{r}_1, \vec{r}_2, \vec{r}_3, \ldots, \vec{r}_N) = \frac{1}{\sqrt{N_e!}} \begin{bmatrix} \psi_1(\vec{r}_1) & \psi_1(\vec{r}_2) & \psi_1(\vec{r}_3) & \cdots & \psi_1(\vec{r}_N) \\ \psi_2(\vec{r}_1) & \psi_2(\vec{r}_2) & \psi_2(\vec{r}_3) & \cdots & \psi_2(\vec{r}_N) \\ \psi_3(\vec{r}_1) & \psi_3(\vec{r}_2) & \psi_3(\vec{r}_3) & \ldots & \psi_3(\vec{r}_N) \\ \vdots & \vdots & \vdots & \ddots & \vdots \\ \psi_N(\vec{r}_1) & \psi_N(\vec{r}_2) & \psi_N(\vec{r}_3) & \cdots & \psi_N(\vec{r}_N) \end{bmatrix} \ldots\ldots (3.5)$$

Where $\frac{1}{\sqrt{N_e!}}$ denotes a normalization factor.

4- Density Functional Theory (DFT)

The aim behind Density Functional Theory (DFT) is to rewrite the Hamiltonian of the electron using electron density rather than wave functions. Researchers like Dirac [9], Slater [10], Hohenburg, and Kohn [11] have made significant contributions to this theory through their theoretical work. The (DFT) theory was first discovered in the works of Thomas and Fermi in 1927[13,4], where they created the main idea in expressing the total energy of an electronic system as a function of electron density by considering the electronic system as a homogeneous and regular gas of electrons where the continuous partitioning of the Brillouin area (without taking into consideration electron correlations) was carried out by the two scientists Thomas and Fermi in order to achieve regions where the electron density is constant in each part. The following two formulas it used to describe the density and kinetic energy of a homogeneous electronic gas:

$$\rho = \frac{1}{3\pi^2} E_f^{\frac{3}{2}} \left(\frac{2m_e}{h^2}\right)^{\frac{3}{2}} \ldots\ldots\ldots (4)$$

$$E_c = \frac{3}{5}\left(\frac{h^2}{2m_e}\right)(3\pi^2)^{\frac{2}{3}}\rho^{\frac{5}{2}} \ldots\ldots\ldots (4.1)$$

The following table provides a comparison between Hartree-Fock method and density functional theory and the characteristics of each method [2].

Table I. 1: Comparison between the two methods, Hartree-Fock and the Density Functional Theory (DFT)[14,15].

HF method	DFT
$\Psi(r)$ 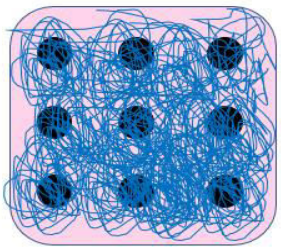	$E[\rho(r)]$ 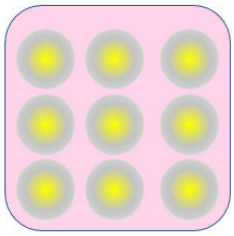
• Principle: Solving the Schrödinger equation by considering the wave functions as a variable basic. • Based on the theory of the mean field theory (MFT). • Calculates wave functions and eigenvalue energy to obtain ground state energy. • Depend on the large number of variables, which makes the equation very complicated and time consuming. • The wave functions obtained as solutions for the Schrödinger equation have no physical meaning. • Does not take into account the correlation terms.	• Principle: Solving the Schrödinger equation by considering the electron density as a variable basic. • Based on the two Hohenburg – Sham theorems and shifting from the Schrödinger equation to the Kohn-Sham equations to find the solution. • Use electron density which has physical meaning. • Reduce the number of variables which makes the equation simpler and faster compared to the HF method. • Used to treat the correlation terms.

4-1 Formalism of Density Functional Theory (DFT)

The densityfunctionaltheory (DFT) is based on describing the total energy of a system with many interacting electrons as a function of the electronic density, rather than its wave function, where the electronic density is expressed by the formula:

$$\rho(\vec{r}) = \sum_{i=1}^{N} |\Psi_i(\vec{r})|^2 \cdots\cdots\cdots (4.2)$$

The Density Functional Theory (DFT) is based on two main theorems:

I. The Theorems of Hohenburg and Kohn

The pair of theorems introduced by Hohenburg and Kohn in 1964 are widely regarded as the foundational pillars of density functional theory.

A-1) First theorem:

The total energy of an electronic system is a functional of the electron density for an external potential V (r), so it is possible to know all the properties of the system when determining the electron density[2,16].

$$E[(\vec{r})] = F[(\vec{r})] + \int V(\vec{r})(\vec{r})dr^3 \ \ldots\ldots\ldots (5)$$

Where F [ρ] is universal functional.

The external potential and the universal functional F [ρ] are expressed in the form:

$$V_{ext}(\vec{r_i}) = -\sum_{A} \frac{Z_A}{r_{iA}} \ldots\ldots\ldots (5.1)$$

$$F[\rho] = T[\rho] + U[\rho] \ldots\ldots\ldots (5.2)$$

Where Z_A is the charge of the nucleus, r_{iA} is the distance between nucleus A and electron i.

A-2) Second theorem:

The second theory appears that to obtain the total energy of the ground state of the electronic system, it is enough to find the corresponding electron density which makes the density function at its minimum value.

$$E\left(\rho_0(\vec{r})\right) \leq E[\rho(\vec{r})] \dots\dots\dots (5.3)$$

$$E(\rho_0) = MinE(\rho) \lim_{\rho \to N} \left\langle \Psi \middle| \hat{T} + \sum_i V_{ext} + V_{ee} \middle| \Psi \right\rangle \dots\dots\dots\dots (5.4)$$

We can get the corresponding electron density of the ground state, by applying the variational principle via the differential of total energy in terms of electron density:

$$\frac{dF[\rho(r)]}{d\rho(r)} + V(r) = 0 \dots\dots\dots\dots (5.5)$$

Therefore, if the electron density which minimizes the energy function is known, we can easily determine the wave function and the exact energy of the ground state.

II. The Kohn - Sham equation

Expressing the kinetic energy and electron-electron interactions analytically in terms of electron density poses a significant challenge when studying many-electron systems. In 1965, Kohn and Sham proposed a pioneering concept to address this challenge. They suggested the notion of substituting the actual electronic system with a hypothetical system where each electron's behavior is treated as independent and uninfluenced by the actions of other electrons. It is only affected by the effective potential (Kohn-Sham potential), which involves both the external potential created by the nuclei's influence and the potential caused by the remaining particles effect on this electron[2,17,18].

The fictive system proposed by Kohn-Sham is characterized by:

- ✓ The Kohn-Sham orbits which are space wave functions of a single electron are solutions of the Schrödinger equation in this vacuum space.
- ✓ The fictive electronic system has the same electronic density as a real system.

- ✓ The kinetic energy of the fictive system is the kinetic energy of the electrons without the correlation effect and it is positive, while the kinetic energy in the real system "T_R" is the sum of the kinetic energy of the fictive system "T_f" and an additional term that expresses the effect of the correlation "T_c" on the kinetic energy of the electron [3] that is:

$$T_R = T_f + T_c \dots\dots\dots\dots (6)$$

$$T_c = \langle \Psi | T | \Psi \rangle - \langle \varphi | T_s | \varphi \rangle \dots\dots\dots\dots (6.1)$$

The V_{ee} interaction between electrons in the real system which is written in the following relation:

$$\langle \Psi | V_{ee} | \Psi \rangle = U_H + U_x + U_c \dots\dots\dots\dots (6.2)$$

where the terms represent:

U_H: The electronic Coulomb (Hartree potential)

U_x: The exchange energy between electrons of the same spin.

Uc: The correlation energy between the electrons.

The Kohn-Sham equation for an electronic system is given as a function of the kinetic energy of the electron: external potential energy, Hartree interaction and exchange-correlation energy as follows:

- ✓ The kinetic energy of an electron in a fictitious system:

$$T_s[\rho] = \left\langle \varphi_i \left| -\frac{\hbar^2}{2\mathrm{m}} \Delta \right| \varphi_i \right\rangle = -\frac{\hbar^2}{2\mathrm{m}} \sum_{\mathrm{i}} \int \varphi_i \nabla^2 \varphi_i^* dr_i \dots\dots\dots\dots (6.3)$$

- ✓ The external potential generated by the effect of nuclei (nucleus-electron interaction):

$$V_{NE}[\rho] = -\int \sum_{I,i} \frac{Z_I \rho(\vec{r})}{\left| \vec{R}_{\mathrm{I}}^{\,0} - \vec{r} \right|} dr \dots\dots\dots\dots (6.4)$$

- ✓ The Hartree potential (Coulomb electron-electron interaction)

$$U[\rho] = \frac{1}{2}\int \frac{\rho(\vec{r})\rho(\overrightarrow{r'})}{|\vec{r} - \overrightarrow{r'}|} dr dr' \dots\dots\dots (6.5)$$

- ✓ The exchange-correlation energy, which is the sum of the correlation and exchange terms, it does not have an exact mathematical expression, but it is estimated by approximations

$$E_{xc}[\rho] = E_x[\rho] + E_c[\rho] \dots\dots\dots (6.6)$$

And finally, the Kohn-Sham equation is written as follows [19–21]:

$$H_{KS}\varphi_i(\vec{r}) = [T_s[\rho] + V_{KS}(\vec{r})]\varphi_i(\vec{r}) = \varepsilon^{KS}\varphi_i(\vec{r}) \dots\dots\dots\dots (6.7)$$

$$V_{KS}(\vec{r}) = V_{ext}(\vec{r}) + V_H(\vec{r}) + +V_{XC}(\vec{r}) \dots\dots\dots\dots\dots (6.8)$$

$$E[\rho] = T_s[\rho] + V_{NE}[\rho] + U_H[\rho] + E_{xc}[\rho] \dots\dots\dots\dots (6.9)$$

B-1) Solution of the Kohn - Sham Equation

Solving the Kohn-Sham equation depends on two basic steps:

• The first step: define all the terms of the effective Kohn-Sham potential, i.e. the exchange-correlation potential E_{xc} must be determined because this term has no mathematical formula but it can be estimated by approximations.

• The second step: find the wave functions (Kohn-Sham orbits), which represent a solutions for the Kohn-Sham equation given by [2]:

$$\varphi_{KS}(\vec{r}) = \sum_j C_{ij}\,\varphi_j(\vec{r}) \dots\dots\dots\dots (6.10)$$

Where $\varphi_i(\vec{r})$ are the basic functions, and Cij are are the development coefficients.

$$\sum_j C_{ij}\, H_{KS}|\varphi_j\rangle = \sum_j C_{ij}\varepsilon_{KS}\,|\varphi_j\rangle \dots\dots\dots\dots (6.11)$$

$$\langle\varphi_k|\sum_j C_{ij}\, H_{KS}|\varphi_j\rangle = \langle\varphi_k|\sum_j C_{ij}\varepsilon_{KS}\,|\varphi_j\rangle \ldots\ldots\ldots\ldots\ldots (6.12)$$

$$\sum_j \quad \big(\langle\varphi_k|H_{KS}|\varphi_j\rangle - \varepsilon_{KS}\langle\varphi_k|\varphi_j\rangle\big)C_{ij} = 0 \ldots\ldots\ldots\ldots (6.13)$$

It remains to determine the C_{ij} coefficients.

The Kohn-Sham equation is solved according to an iterative cycles illustrated by figure (1.I), where the process starts using an initial density $\rho_{in}$for the first iteration, this density is used to solve the Kohn-Sham equation, then, We use a superposition of the atomic densities and we compute the Kohn-Sham matrix, to solve the equations to obtain the Kohn-Sham orbitals.

After this step, we calculate the new densityρ_{out}, to check the convergence condition (if the density or energy has changed a lot or not) and we mixed the two charge densities $\rho_{out}$and ρ_{in}as follow:

$$\rho_{in}^{i+1} = (1-\alpha)\rho_{in}^{i} + \rho_{out}^{i} \ldots\ldots\ldots\ldots (6.14)$$

Thus the iterative procedure can be repeated until the convergence condition is fulfilled.

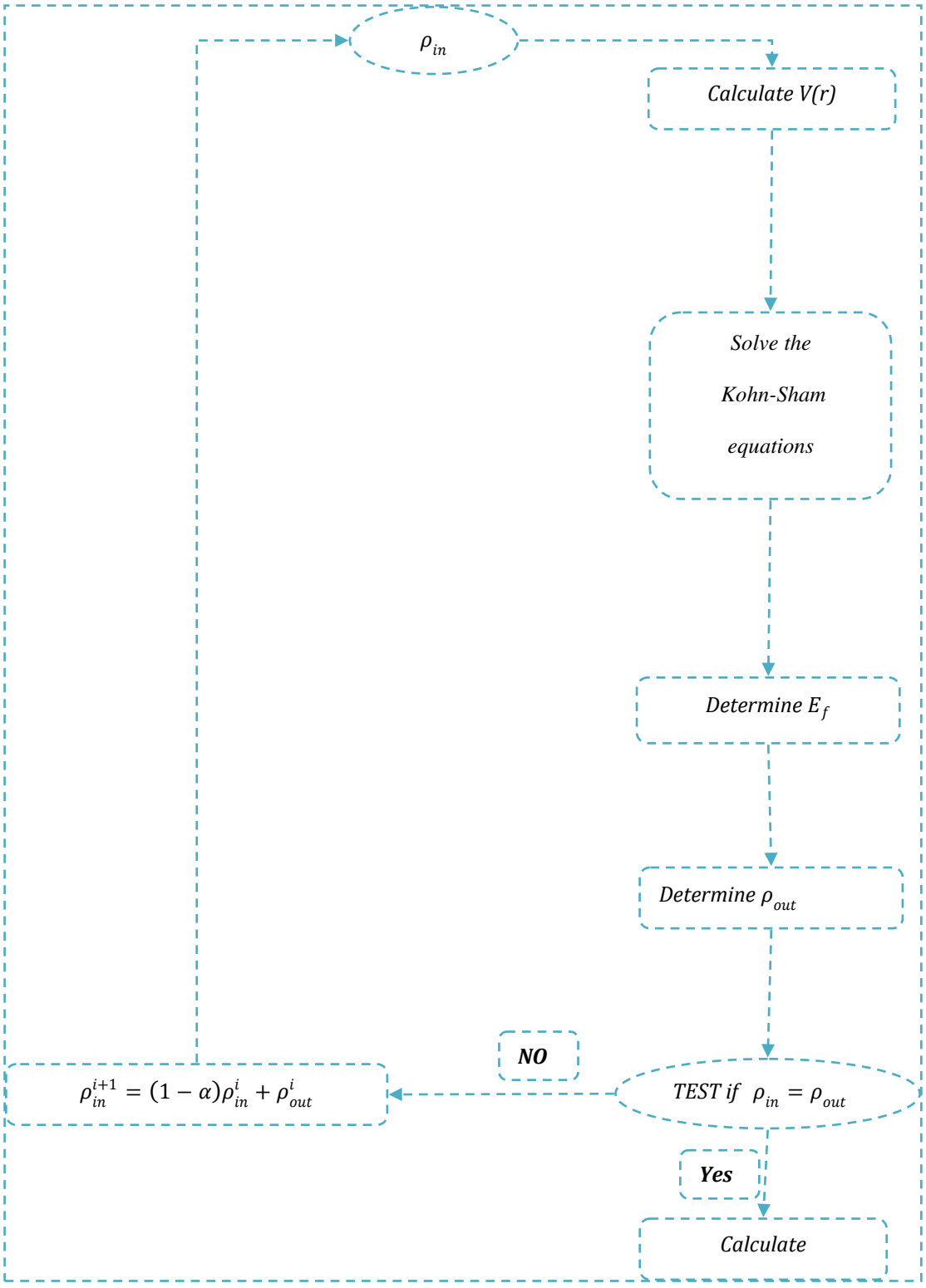

Figure I. 1: Self-consistent calculation flowchart.

5-The Different Types of Approximation of the $E_{xc}[\rho]$

Due to the absence of an analytical expression for the exchange-correlation potential between electrons, various approaches have been devised to approximate its values. The accuracy of the obtained results largely hinges on the mathematical formulation of this potential[2].

5-1 Local density approximation (LSDA)

the local density approximation model was first proposed by Kohn and Sham in 1964 [22]where the inhomogeneous electronic system is approximated by a local homogeneous electronic system after dividing the Brillouin region into small regions, and the expression energy exchange - correlation is given by the relation :

$$E_{XC}^{LSDA} = \int \rho(\vec{r})\, E_{xc}[\rho(\vec{r})] d\vec{r} \ldots\ldots\ldots (7)$$

$$V_{xc} = \frac{dE_{XC}^{LDA}[\rho]}{d\rho} = \varepsilon_{XC}^{LDA} + \rho(\vec{r})\frac{d\varepsilon_{XC}^{LDA}}{d\rho} \ldots\ldots\ldots\ldots (7.1)$$

For each spin up or down magnetic order, the total electron density becomes the sum of the two electron densities

$$\rho(\vec{r}) = \rho_{\uparrow}(\vec{r}) + \rho_{\downarrow}(\vec{r}) \ldots\ldots\ldots (7.2)$$

The Kohn-Sham equation for the two spins in the form [2]:

$$\begin{cases} \left(\frac{-\hbar^2}{2m}\nabla^2 + V_{eff}^{\uparrow}(\vec{r})\right)\varphi_i(\vec{r}) = \varepsilon_{KS}^{\uparrow}\varphi_i(\vec{r}) \\ \left(\frac{-\hbar^2}{2m}\nabla^2 + V_{eff}^{\downarrow}(\vec{r})\right)\varphi_i(\vec{r}) = \varepsilon_{KS}^{\downarrow}\varphi_i(\vec{r}) \end{cases} \ldots\ldots\ldots\ldots\ldots\ldots (7.3)$$

5-2 The Generalized Gradient Approximation GGA

The Generalized Gradient Approximation GGA is a new approximation was developed, in which the localized electron density was considered to be non-homogeneous

and varied from place to place. so, the total energy of the electron system is proportional to both the electron density $\rho(\vec{r})$ and and its gradient $\nabla\rho(\vec{r})$, as shown by the equation[23]:

$$E_{XC}^{GGA}[\rho(\vec{r})] = \int d^3\vec{r}\rho(\vec{r})\varepsilon_{XC}[\rho(\vec{r}), \nabla\rho(\vec{r})] \dots\dots\dots\dots(8)$$

6- Full-Potential Linearized Augmented Plane-wave Method FP-LAPW

Full-Potential Linearized Augmented Plane-wave Method (FP-LAPW) method aimed to look for the wave functions as solutions to the Cohn-Sham equation became necessary. After extensive research, certain approaches emerged, including the OPW method presented by Herring theory in 1940 [24], the LMTO method [25], and the (FP-LAPW) method, where these methods are dependent on the quality of the effective potential utilized.

6-1 The Plane Wave method (APW)

The plane wave method, pioneered by scientist Slater [8], involved dividing the crystal space into distinct regions utilizing the Muffin-Tin approximation [26], as depicted in Figure I.2. This approximation represents atoms as non-overlapping spheres with a radius denoted as R0, within which the core electrons reside. Between these atomic spheres lies an interstitial region hosting free electrons, which are spatially distant from the atomic nuclei.

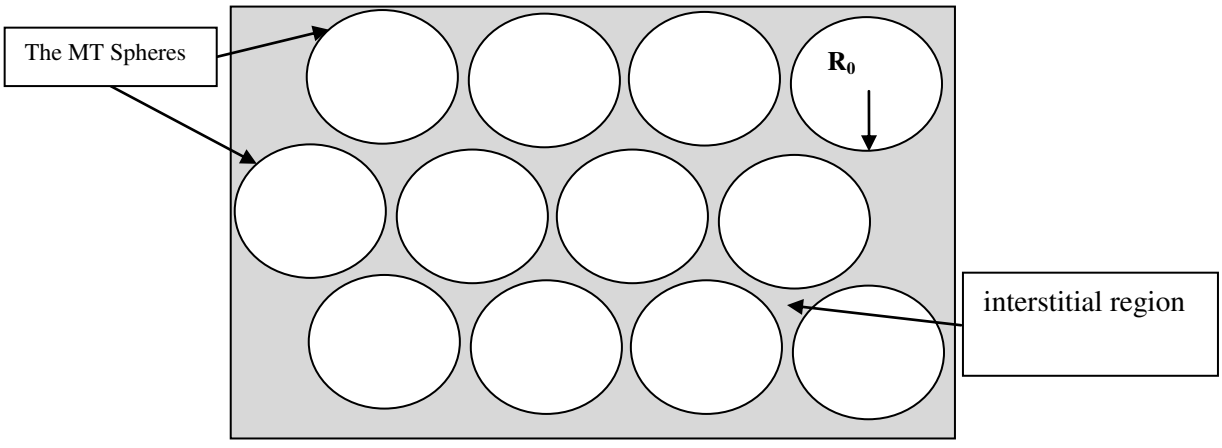

Figure I. 2: Diagram of the distribution of the elementary cell in atomic spheres and in interstitial region.

According to this approximation, the core electrons located inside the sphere are subjected to the spherical potential, on the other hand, in the interstitial region the potential is constant[2]. So, the potential in the two regions is given in the form:

$$V(\vec{r}) = \begin{cases} V(r) & r \leq R_0 \\ 0 & r > R_0 \end{cases} \dots\dots\dots\dots (9)$$

The waves that describe the behavior of electrons inside MT spheres differ from those in the interstitial region, they are described by plane waves in the interstitial region, while inside spheres by functions radials multiplied by spherical harmonics[2]. The two different wave functions are given by the following expression:

$$\varphi(\vec{r}) = \begin{cases} \sum_{l=0}^{\infty} \sum_{-m}^{m} A_{lm} U_l(r) Y_{lm}(r) & r \leq R_0 \\ \frac{1}{\sqrt{\Omega}} \sum_G C_G \, e^{i(\vec{K}+\vec{G})\vec{r}} & r > R_0 \end{cases} \dots\dots\dots\dots\dots (9.1)$$

Where , Ω: The cell volume

Y_{lm}: Spherical harmonics

A_{lm}: Development coefficients

U_l: The regular solution of the Schrödinger equation given by[27]:

$$\left(-\frac{d^2}{dr^2} + \frac{l(l+1)}{r^2} V(\vec{r}) \right) r U_l = E_l U_l \dots\dots\dots\dots\dots (9.2)$$

Where E_l: An energy parameter.

6-2 The Linearized Augmented Plane Wave Method (FP-LAPW)

The darkpoint of using the APW method is its slow process in calculations due to the common radial function U_l; additionally, it is difficult to define the radial function for each value of energy E_l. so that, Anderson [28]made improvements to the APW method [29]by using the Taylor expansion to write the radial functions U_l (r) in the following form:

$$U_l(r,E) = U_l(r,E_l) + (E_l - E) \left. \frac{dU_l(r,E)}{dE} \right|_{E=E_l} + \mathcal{O}(E_l - E)^2 \dots\dots\dots\dots (10)$$

Where the term $\mathcal{O}(E - E_l)^2$ represents the quadratic error.

After several simplifications, he has got the expression of potential inside and outside of Muffin-Tin balls as follows:

$$V(r) = \begin{cases} \sum_{lm}^{m} V_{lm}(r) Y_{lm} & r \leq R_0 \\ \sum_{lm}^{m} V_k(r) e^{ikr} & r > R_0 \end{cases} \quad \ldots\ldots\ldots\ldots\ldots (10.1)$$

As well as the wave functions inside the spheres in terms of radial functions and their derivatives. Where the wave functions are written as follows [30,31]:

$$\Phi_{\vec{K}+\vec{G}}(\vec{r}) = \begin{cases} \sum_{lm} \left(A_{lm} U_l(r) + B_{lm} \dot{U}_l(r) \right) Y_{lm}(r) & r \leq R_0 \\ \frac{1}{\sqrt{\Omega}} \sum_{G} C_G \, e^{i(\vec{K}+\vec{G})\vec{r}} & r > R_0 \end{cases} \quad \ldots\ldots\ldots\ldots (10.2)$$

Where :

$\vec{K}$: represents the wave vector.

$\vec{G}$: is the vector of the reciprocal lattice.

A_{lm}:: are coefficients corresponding to the function U_l.

B_{lm}: are coefficients corresponding to the function U_l.

We can determine the coefficients A_{lm} and B_{lm}, for each wave vector, and for each atom by applying the conditions of continuity of the basic functions in the vicinity of the limit of the spheres. After some simplifications we find the coefficient formula A_{lm} and B_{lm} in the following forms:

$$A_{lm} = \frac{4\pi {r_0}^2 i^L}{\sqrt{\Omega}} {Y^*}_{lm}(K+G) a_l(K+G) \quad \ldots\ldots\ldots\ldots (10.3)$$

$$B_{lm} = \frac{4\pi {r_0}^2 i^L}{\sqrt{\Omega}} {Y^*}_{lm}(K+G) b_l(K+G) \ldots\ldots\ldots\ldots\ldots (10.4)$$

7- WIEN2K SOFTWARE

The wien2k program is composed of numerous subprograms coded in the Fortran language. These subprograms serve as algorithms tasked with translating the equations governing the behavior of crystalline systems, particularly those processed using density functional theory (DFT). Within this framework, the program adopts the full potential

linearized augmented plane wave (FP-LAPW) method as its computational approach. This method serves as a sophisticated tool for calculating various properties of compounds under study, offering insights into their structural, electronic, and energetic characteristics. [2].

The most important subprograms and their roles in the Wien2k program [32] are indicated in the diagram presented in Figure I.3 and are organized as follows: [2]:

- ❖ NN: This subprogram calculates distances between nearest neighbors up to a specified limit, thus helping to determine the value of the atomic sphere radius.
- ❖ SGROUP: Determines the space group of the compound.
- ❖ SYMMETRY: A program that determines the symmetry number and symmetry operations of the space group of our structure.
- ❖ LSTART: Computes electron densities of free atoms and determines how different orbitals will be treated in band structure calculations.
- ❖ KGEN: Generates a mesh of K points in the irreducible part of the first Brillouin zone (1st BZ). The number of K points in the entire 1st BZ is specified.
- ❖ DSTART: Produces an initial density for the self-consistent field (SCF) cycle by superimposing atomic densities produced in the LSTART subprogram.

After the last subprogram, we enter into a loop of SCF calculations and consequently proceed to the following five steps:

- ✓ LAPW0 (POTENTIAL): Uses the total electron density to calculate the Coulomb and exchange potentials (Hartree-Fock potential). Additionally, it divides space into a muffin-tin (MT) sphere and an interstitial region.
- ✓ LAPW1 (BANDS): Calculates eigenvalues and wave functions for valence electrons from the solution of equation (III.1).
- ✓ LAPW2 (RHO): Calculates valence electron densities obtained in the LAPW0 step.
- ✓ LCORE: Computes eigenvalues and wave functions to obtain core electron densities.
- ✓ MIXER: Computes the new density through mixing.

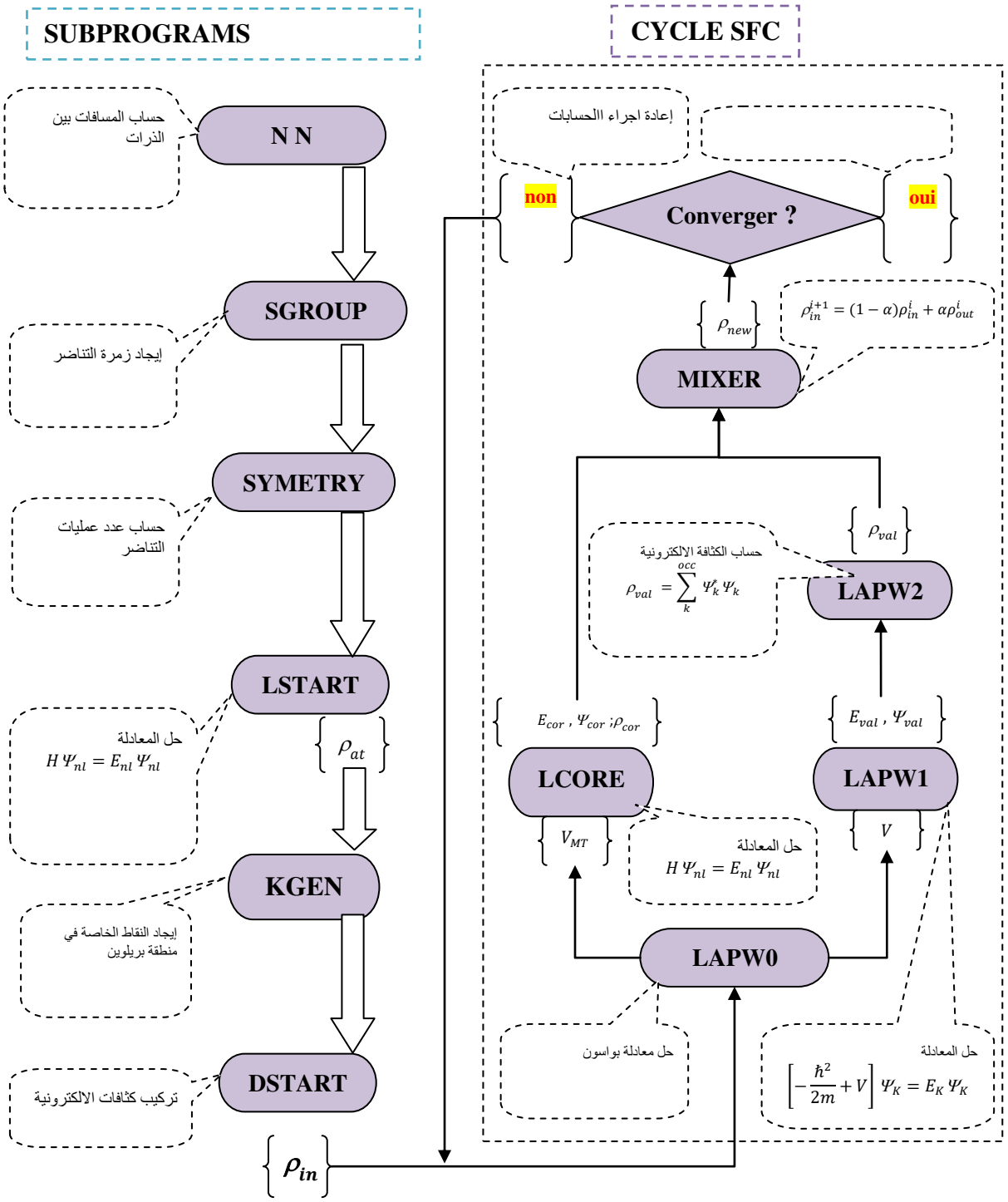

Figure I. 3: Subprograms integrated in the wien2k code [2].

References

[1] S.S. Essaoud, M. Imadalou, D.E. Medjadi, Microscopic Study of Correlations in Finite Fermionic Systems by Breaking the Axial Symmetry, Int J Mod. Theo Phys. 5 (2016) 8–21.

[2] S. Saad Essaoud, Les composés à base de manganèse: investigation théorique des propriétés structurales électroniques et magnétiques, DOCTORAT THESIS, 2020. https://doi.org/10.13140/RG.2.2.30742.68169.

[3] S. Saad Essaoud, Etude microscopique des corrélations dans les systèmes fermioniques finis en brisant la symétrie axiale, 2013. https://doi.org/10.13140/RG.2.2.19283.71203.

[4] M. Born, R. Oppenheimer, Zur Quantentheorie der Molekeln, Ann. Phys. 389 (1927) 457–484. https://doi.org/10.1002/andp.19273892002.

[5] D.R. Hartree, The wave mechanics of an atom with a non-coulomb central field. Part II. Some results and discussion, in: Math. Proc. Camb. Philos. Soc., Cambridge University Press, 1928: pp. 111–132.

[6] D.R. Hartree, The wave mechanics of an atom with a non-coulomb central field. part iii. term values and intensities in series in optical spectra, in: Math. Proc. Camb. Philos. Soc., Cambridge University Press, 1928: pp. 426–437.

[7] V. Fock, „Selfconsistent field “mit Austausch für Natrium, Z. Für Phys. 62 (1930) 795–805.

[8] J.C. Slater, Damped Electron Waves in Crystals, Phys. Rev. 51 (1937) 840–846. https://doi.org/10.1103/physrev.51.840.

[9] P.A.M. Dirac, Note on Exchange Phenomena in the Thomas Atom, Math. Proc. Camb. Philos. Soc. 26 (1930) 376–385. https://doi.org/10.1017/S0305004100016108.

[10] J.C. Slater, A Simplification of the Hartree-Fock Method, Phys. Rev. 81 (1951) 385–390. https://doi.org/10.1103/PhysRev.81.385.

[11] P. Hohenberg, W. Kohn, Inhomogeneous Electron Gas, Phys. Rev. 136 (1964) B864–B871. https://doi.org/10.1103/physrev.136.b864.

[12] L.H. Thomas, The calculation of atomic fields, Math. Proc. Camb. Philos. Soc. 23 (1927) 542. https://doi.org/10.1017/s0305004100011683.

[13] E. Fermi, Eine statistische Methode zur Bestimmung einiger Eigenschaften des Atoms und ihre Anwendung auf die Theorie des periodischen Systems der Elemente, Z. Für Phys. 48 (1928) 73–79.

[14] ل. مروة, دراسة الخواص الكهرو حرارية والترموديناميكية للمركب CsVO3, Master Thesis, UNIVERSITE MOHAMED BOUDIAF-M'SILA, 2021.

[15] آ. قريشي, دراسة نظرية للخواص البنيوية، الإلكترونية والضوئية للمركبين AgMgF k3MgF, Master Thesis, UNIVERSITE MOHAMED BOUDIAF-M'SILA, 2021.

[16] R.M. Dreizler, E.K.U. Gross, Density Functional Theory, (1990). https://doi.org/10.1007/978-3-642-86105-5.

[17] R. Stowasser, R. Hoffmann, What do the Kohn- Sham orbitals and eigenvalues mean?, J. Am. Chem. Soc. 121 (1999) 3414–3420.

[18] A. Seidl, A. Görling, P. Vogl, J.A. Majewski, M. Levy, Generalized Kohn-Sham schemes and the band-gap problem, Phys. Rev. B 53 (1996) 3764.

[19] C. Fiolhais, F. Nogueira, M.A. Marques, A primer in density functional theory, Springer Science & Business Media, 2003.

[20] F.M. Bickelhaupt, E.J. Baerends, Kohn-Sham density functional theory: predicting and understanding chemistry, Rev. Comput. Chem. 15 (2000) 1–86.

[21] J.A. Pople, P.M. Gill, B.G. Johnson, Kohn—Sham density-functional theory within a finite basis set, Chem. Phys. Lett. 199 (1992) 557–560.

[22] W. Kohn, L.J. Sham, Self-Consistent Equations Including Exchange and Correlation Effects, Phys. Rev. 140 (1965) A1133–A1138. https://doi.org/10.1103/physrev.140.a1133.

[23] D.M. Ceperley, B.J. Alder, Ground State of the Electron Gas by a Stochastic Method, Phys. Rev. Lett. 45 (1980) 566–569. https://doi.org/10.1103/physrevlett.45.566.

[24] C. Herring, A new method for calculating wave functions in crystals, Phys. Rev. 57 (1940) 1169.

[25] H.L. Skriver, The LMTO Method: Muffin-Tin Orbitals and Electronic Structure, Springer-Verlag, Berlin Heidelberg, 1984. https://doi.org/10.1007/978-3-642-81844-8.

[26] O.K. Andersen, T. Saha-Dasgupta, Muffin-tin orbitals of arbitrary order, Phys. Rev. B 62 (2000) R16219.

[27] D D Koelling and G O Arbman, Use of energy derivative of the radial solution in an augmented plane wave method: application to copper, J. Phys. F Met. Phys. 5 (1975) 2041.

[28] O.K. Andersen, Linear methods in band theory, Phys. Rev. B 12 (1975) 3060–3083. https://doi.org/10.1103/physrevb.12.3060.

[29] M. Petersen, F. Wagner, L. Hufnagel, M. Scheffler, P. Blaha, K. Schwarz, Improving the efficiency of FP-LAPW calculations, Comput. Phys. Commun. 126 (2000) 294–309.

[30] D.R. Hamann, Semiconductor Charge Densities with Hard-Core and Soft-Core Pseudopotentials, Phys. Rev. Lett. 42 (1979) 662–665. https://doi.org/10.1103/physrevlett.42.662.

[31] M. Weinert, Solution of Poisson's equation: Beyond Ewald-type methods, J. Math. Phys. 22 (1981) 2433–2439. https://doi.org/10.1063/1.524800.

[32] P. Blaha, K. Schwarz, G. Madsen, D. Kvasnicka, J. Luitz, Wien2k, (2001).

the chapter 2:

CALCULATING THE PROPERTIES OF $CoAgF_3$ and $FeAgF_3$ COMPOUNDS

CHAPTER 2:

CALCULATING THE PROPERTIES OF $CoAgF_3$ and $FeAgF_3$ COMPOUNDS

1- Introduction

In this chapter, our focus delves into scrutinizing the structural properties of $CoAgF_3$ and $FeAgF_3$ compounds by employing the theoretical frameworks elucidated earlier. Initially, we embark on calculating pivotal parameters such as the bulk modulus, lattice constant, energy, and unit cell volume at their ground states. This meticulous analysis lays the groundwork for comprehending the fundamental structural dynamics of these materials.

Subsequently, our investigation extends to exploring the electronic behavior inherent in both compounds. We meticulously compute the band structure alongside the total and partial density of states. This in-depth examination offers valuable insights into the intricate electronic characteristics exhibited by $CoAgF_3$ and $FeAgF_3$.

Furthermore, by deciphering the distinctive attributes of these substances, we aim to discern their optimal industrial applications. Identifying the most suitable sectors for their utilization and discerning the ideal operational conditions can significantly enhance productivity and foster favorable outcomes. Through this comprehensive study, we endeavor to provide guidance for leveraging the unique properties of $CoAgF_3$ and $FeAgF_3$ in diverse industrial settings, thereby maximizing their potential and ensuring beneficial outcomes.

2- Computational details

The structural, electronic and magnetic findings obtained in this work were calculated using the method of linearly increasing waves and full potentials [1–6] FP-LAPW integrated into the WIEN2k simulation program [7] based mainly on density theory, where we used the generalized gradient approximation to treat the exchange-correlation potential. (GGA-PBEsol) [9] in estimating the structural and magnetic properties, while we used the modified Becke Johnsson approximation (mBJ) [10] to predict the electronic properties of both compounds.

During the phases of the completed work, we applied the Muffin-Tin approximation [11] and divided the space into two regions:

- **The first area:** We considered atoms as spheres with radii **Rmt**, where the wave function inside them is described by spherical harmonic functions with a maximum angular moment **lmax**. For the two compounds that we studied, we took the values of 2.3 a.u. for the Ag atom, 2.1 a.u. for the Co and Fe atoms, and 1.6 a.u. for the oxygen atom F as the radii of the constituent atoms, with the necessity of the presence of the internal electrons "the core electrons" inside these balls in a way that does not cause interference between these balls.
- **The second region:** It is the interstitial region that represents the remaining space of the first region, i.e. the interstitial spaces, and the wave function is in it as plane waves with a cutoff coefficient **Kmax × RMT**, where **RMT** is the average radius of the **Muffin-Tin** balls and **Kmax** is the maximum value of the wave vector coefficient for the quasi-inverse, where it was chosen. The optimal value of the cutting factor **Kmax RMT = 8** and Kpoint equals 1000. We point out that the criterion and condition of convergence for

the total energy in all calculations performed for both compounds and using both approximations is equal to 10^{-4} **Ry**. The electronic distribution of the atoms forming the two compounds was as follows:

Fe → [Ar] $4S^2$ $3d^6$

F → [He] $1S^2 2S^2$ $2p^5$

Co → [Ar] $4S^2$ $3d^7$

Ag → [Kr] $4d^{10} 5S^1$

3- Results and discussion

3.1- Structural properties:

We studied both the compounds $CoAgF_3$ and $FeAgF_3$, which belong to the perovskite family. the two compounds $CoAgF_3$ and $FeAgF_3$ crystallize in the cubic structure as shown in Figure (II.2), which was drawn using the VESTA program [12–15]. According to the image, the crystal cell consists of five atoms occupying Wyckoff positions. next :

Ag: (0.5 0.5 0.5)

Fe or Co: (0 0 0)

F:(0.5 0 0) (0 0 0.5) (0 0.5 0)

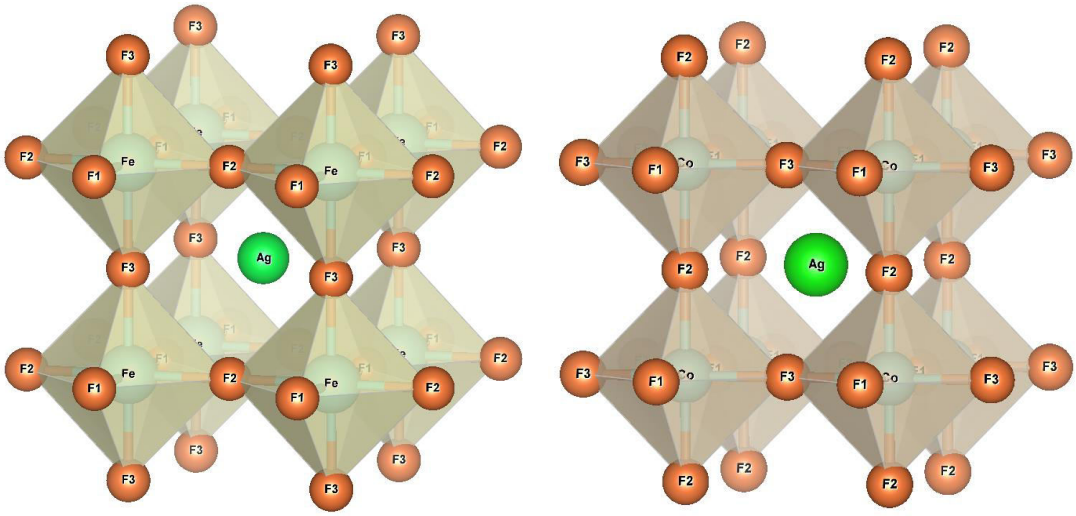

Figure (II.1): Crystal structure of **$CoAgF_3$** and **$FeAgF_3$** (made using **VESTA** program).

When calculating the structural properties of the compounds **$CoAgF_3$** and **$FeAgF_3$**, we calculated the total energy changes of the primary cell at different sizes, using **GGA** approximations in the case **ferrmagnetic (FM)**.

the volume- energy curves for both compounds are plotted based on Murnaghan equation [16] expressed by the following relationship:

$$\mathrm{E(V)} = E_0 + \frac{B}{B'(\mathrm{B}' - 1)}\left[V\left(\frac{V_0}{V}\right)^{\mathrm{B}'} - V_0\right] + \frac{B}{B'}(V - V_0) \dots\dots\dots\dots (\mathrm{II})$$

So that it represents transactions

V_0: cell volume at equilibrium.

E_0: The total energy of the primary cell in equilibrium.

B: Coefficient of compressibility

B': The first derivative of the bulk modulus

in figures II.2 and II.3, we plotted the two curves of the total energy changes of the crystal cell as a function of volume for the ferromagnetic states (**FM**) in order to determine the equilibrium state for the compounds **$CoAgF_3$** and **$FeAgF_3$**.

After determining the most stable state for both compounds **$CoAgF_3$** and **$FeAgF_3$**, we calculated some structural properties such as cell constant, bulk modulus and its derivative, minimum energy, and lattice constant parameter, as shown in **Tables (II.1)** and **(II.2).** As an analysis of the

results obtained in the two tables, we note that the compound **$FeAgF_3$** has a crystal cell constant **a(Å)** greater than the compound **$CoAgF_3$** at equilibrium (the most stable state), and it should be noted that the values we obtained using the **GGA** approximation for both compounds were very close to the results obtained. It has been found in other research [17,18].

. Regarding the bulk modulus, knowing its value gives an clear idea about the highest pressure value that the material can exposed without causing it to deform. Through the results obtained, we found that the compound **$FeAgF_3$** has a greater compressive modulus value than the compound **$CoAgF_3$**, and therefore it is more resistant to pressure.

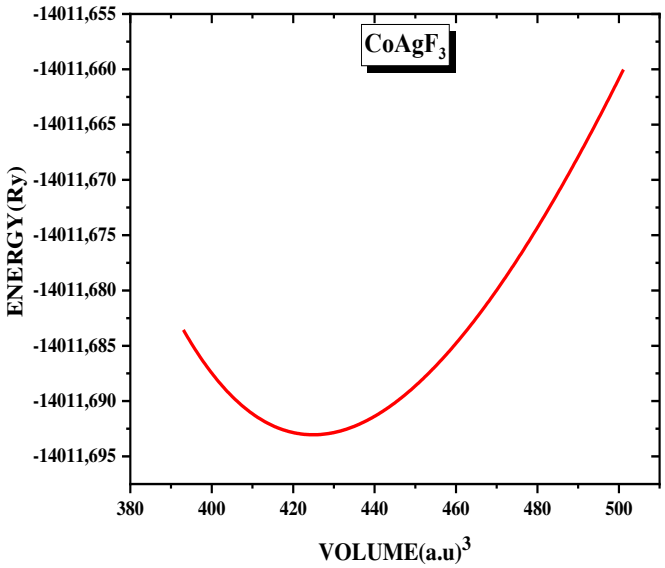

Figure (II.2): Changes in the total energy of the compound **$CoAgF_3$** as a function of changes in the volume of the crystal cell.

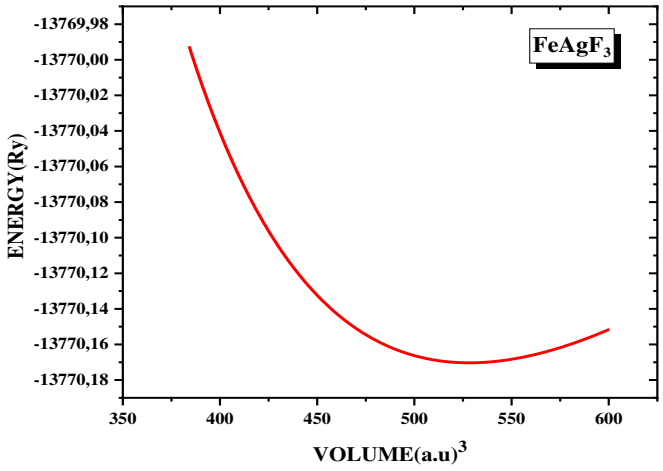

Figure (II.3): Changes in the total energy of the compound $FeAgF_3$ as a function of changes in the volume of the crystal cell.

Table (II.01): Values of the structural properties of the compound $FeAgF_3$ calculated using the GGA approximation

$FeAgF_3$	V_0 (a.u)^3	528.2612	4.196[1]
	E_{mini} (Ry)	-13770.1703	
	a(Å)	4.2778	
	B(GPa)	70.9009	
	B'(GPa)	4.5304	

Table (II.02): Values of the structural properties of the compound $CoAgF_3$ calculated using the GGA approximation

$CoAgF_3$	V_0 (a.u)^3	424.9285	
	E_{mini} (Ry)	-14011.693	
	a(Å)	3.9784	**3.983**[1] **3.955**[2]
	B(GPa)	98.6783	
	B'(GPa)	5.2377	

4- Magnetic properties

The magnetic properties exhibited by materials hold significant relevance across various industrial sectors. Prior to delving into their study, it is imperative to grasp the underlying origins and mechanisms driving magnetic behavior within solid compounds, as highlighted by previous research [19–27]. Hence, our exploration will commence with a comprehensive overview delineating the fundamental sources of magnetic behavior in materials. This overview will be structured across three distinct levels, facilitating a nuanced understanding of the intricate processes governing magnetism within solid compounds.

4-1- The first level (electron level):

The electron possesses a magnetic moment stemming from its dual rotational motions, both around its own axis and around the nucleus within an atom. These rotations engender two distinct types of magnetic moments. Firstly, there's the spin magnetic moment, which can be quantified by the following expression:

$$\vec{\mu}_s = -g \frac{\mu_B}{\hbar} \vec{S} \ldots\ldots\ldots\ldots (\mathbf{II.1})$$

And an orbital magnetic moment $\vec{\mu}_{sI} = \frac{\mu_B}{\hbar} \vec{I}$

• As shown in **Figure (II.02):**

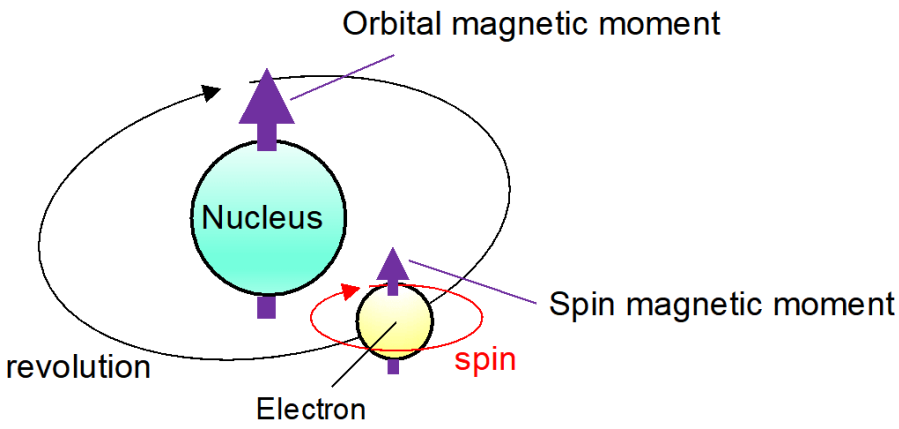

Figure (II.04): The spin and orbital magnetic moments of the electron.

4-2- The second level (the level of atoms):

The magnetic state of an atom and the arrangement of its electrons in the outer orbit are regulated by these magnetic moments. When all electrons are arranged in a paired manner, with their spins oriented oppositely—one upward and the other downward—the atom exhibits non-magnetic behavior. This occurs because the sum of the magnetic moments of the electrons cancels out, resulting in a net magnetic moment of zero. A prime illustration of this can be observed in the configuration of a zinc atom, as depicted in Figure (II 5-a(

Conversely, when electrons in the outer orbit are positioned individually, the atom adopts a magnetic character. This is illustrated by the nitrogen atom shown in Figure (II 5-b). In such cases, the magnetic moments of the unpaired electrons do not fully cancel each other out, resulting in a net magnetic moment, thereby rendering the atom magnetic.

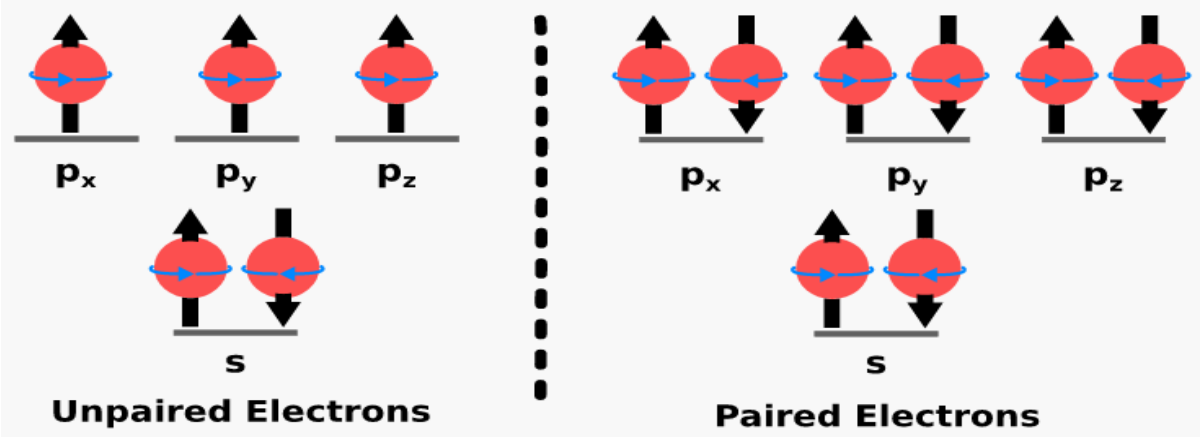

B - Example of a nitrogen atom **A - Example of a zinc atom**

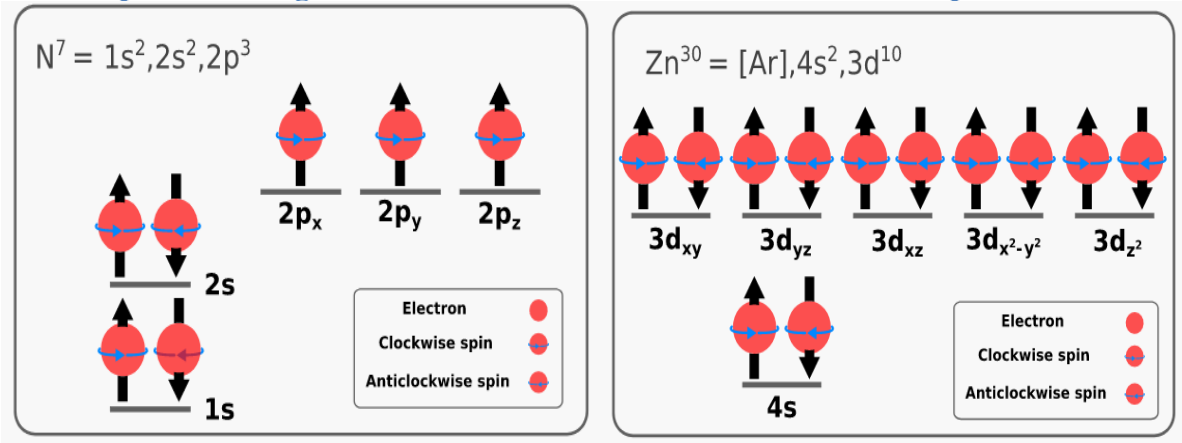

Figure II.5: The origin of magnetic behavior in magnetic and non-magnetic atoms

4-3- The third level (matter level):

The magnetic state of matter is influenced by a multitude of factors, with the primary determinants being the intrinsic magnetic properties of the constituent atoms (whether they are magnetic or non-magnetic), the interatomic distances, and the exchange interactions among them. Additionally, the influence of temperature and the presence of an external magnetic field play pivotal roles in shaping the magnetic behavior of matter.

The magnetic interactions between atoms, crucial in understanding magnetic states, are governed by exchange interactions. These interactions are intimately tied to the magnetic moments of the atoms, the spatial separation between them, and the influence of any external magnetic fields they encounter [20].

Describing these interactions, Heisenberg introduced a Hamiltonian, which provides a mathematical framework for understanding the interplay of these factors. The Hamiltonian expression elucidates the intricate relationship between magnetic moments, interatomic distances, and the impact of external magnetic fields, offering valuable insights into the magnetic properties of matter.

$$H_{mag} = \sum_{i\,j} J_{ij}\vec{S}_i.\vec{S}_j \; + \sum_i g_i\mu_B\,\vec{h}\;\;\vec{S}_i \ldots\ldots\ldots\ldots\ldots (\text{II. 3})$$

Where $\boldsymbol{\mu_B}$ represents the Bohr magne, $\boldsymbol{g_i}$ is the magnetic constant, $\boldsymbol{\vec{S}_i}$ spin magnetic moment beam, $\boldsymbol{\vec{h}}$ is the external magnetic field, and $\boldsymbol{J_{ij}}$ is a coupling constant for the exchange reaction which is an integral.

Materials are classified according to their magnetic features into five categories represented in **Figure (II.6)**, which are as follows:

a. **Diamagnetic materials:** They consist of non-magnetic atoms. This is because all the electrons in the outer orbit of the atoms that make them up are in a two-paired state, and thus the sum of the electrons' moments is zero [19–23,28].

b. **Paramagnetic materials:** They consist of magnetic atoms, each of which contains unpaired electrons in its outer orbit. Given that the distances between the atoms are large, no exchange interaction occurs between the magnetic moments of the electrons (atoms),

and therefore the magnetic moments will move randomly, and the total sum of the magnetic moments of the atoms will be zero [19 -23,28].

c. **Ferromagnetic materials:** They consist of magnetic atoms, each of which contains electrons in its outer orbit. Due to the fact that the distances between the atoms are small, the coupling coefficient between the magnetic moments of the electrons, J_{ij} , is negative, and thus the magnetic moments move in parallel, and the total moment of the compound is a non-zero sum of the magnetic moments of the atoms [19–23,28].

d. **Antiferromagnetic materials:** They consist of magnetic atoms, each of which contains electrons in its outer orbit, and because the distances between the atoms are very small, the coupling coefficient between the magnetic moments of the electrons J_{ij} is positive, and therefore the magnetic moments will be directed in opposite directions (one up and the other down), and because the atoms composing the compound They have magnetic moments that are equal in value and opposite in direction, so the total sum of the magnetic moments of the atoms is zero [19–23,28].

e. **Ferrimagnetic materials:** They are an intermediate state between the antimagnetic state and the paramagnetic state, as they consist of magnetic atoms. The coupling coefficient between the magnetic moments of the electrons, J_{ij}, is negative, and thus the magnetic moments go in opposite directions (one up and the other down), and because the atoms have opposite magnetic moments in the direction... Their value is equal, so the total sum of the magnetic moments of the atoms is non-zero [19–23,28].

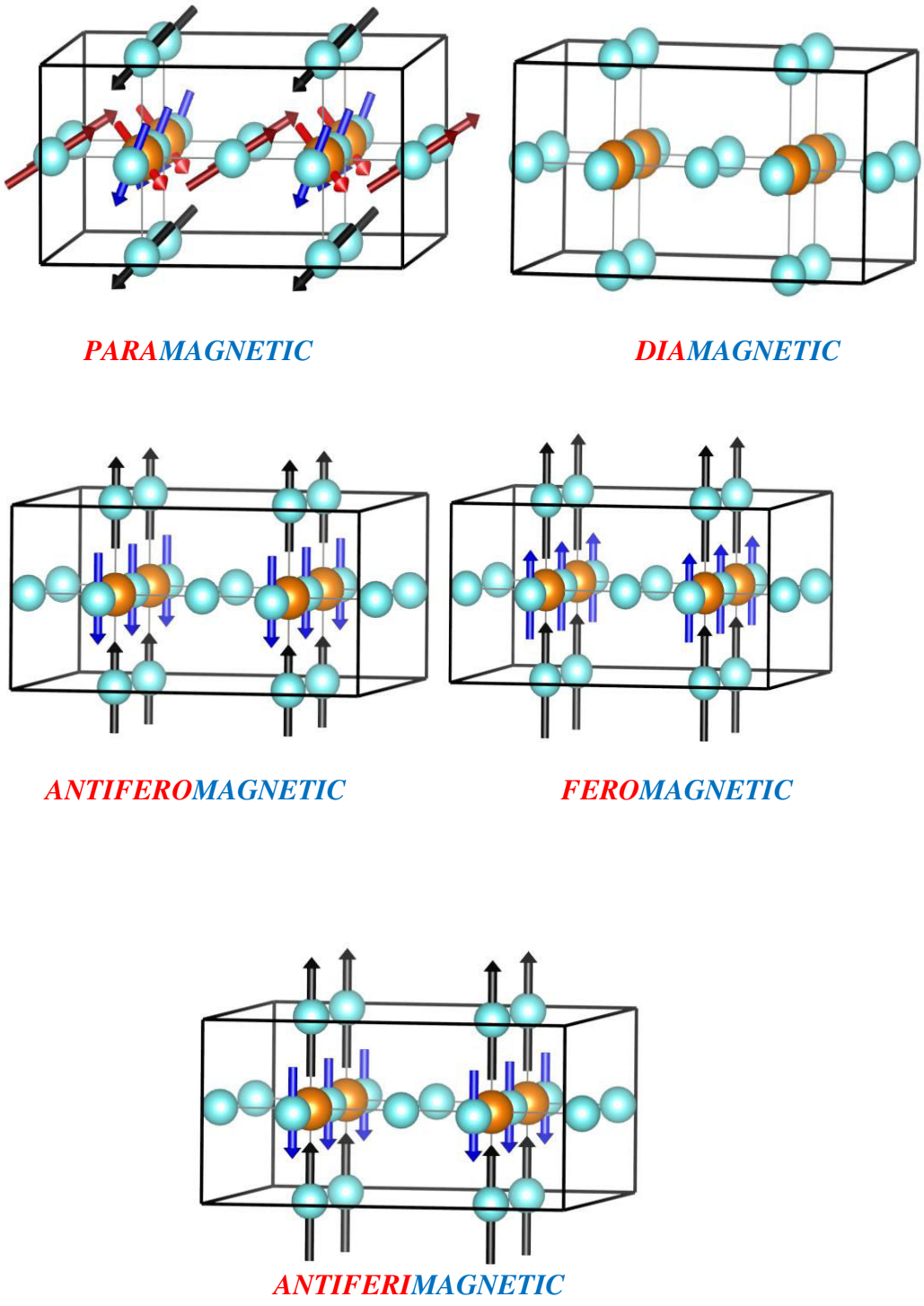

Figure (II.6): Classification of materials according to their magnetic state

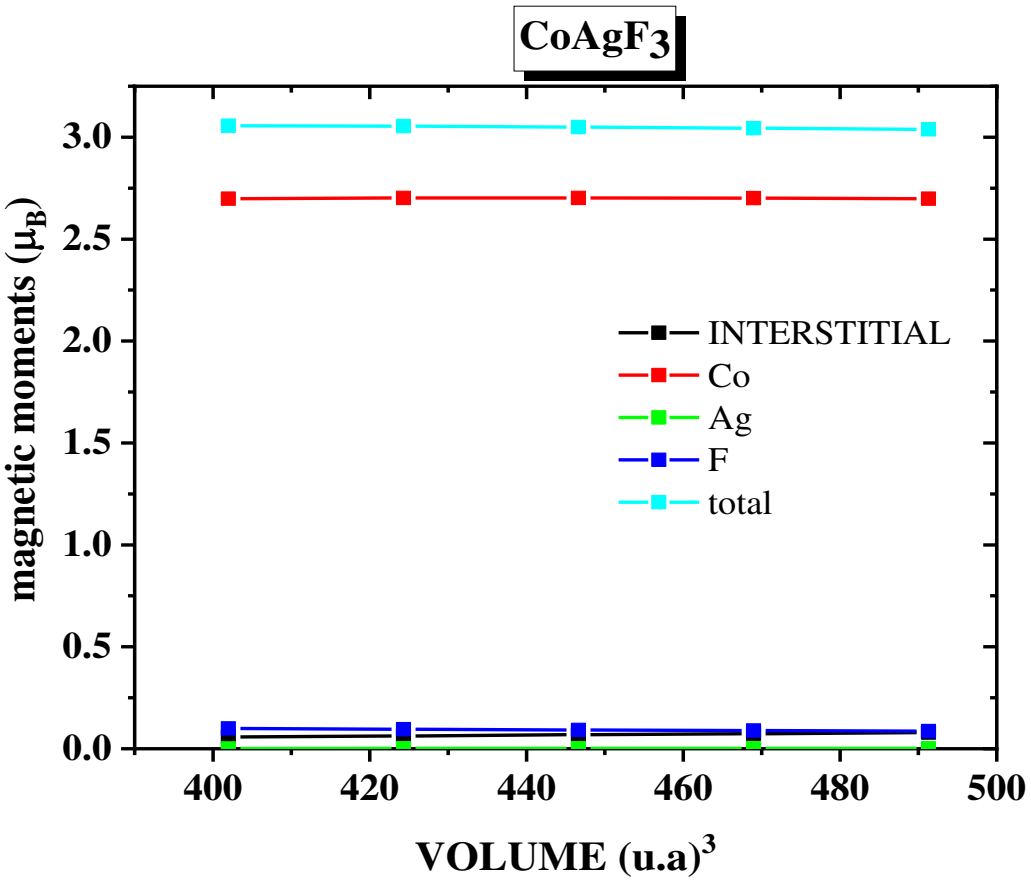

Figure II.7: Changes in the total and molecular magnetic moments of the compound **$CoAgF_3$** as a function of changes in the unit cell volume using the **GGA** approximation.

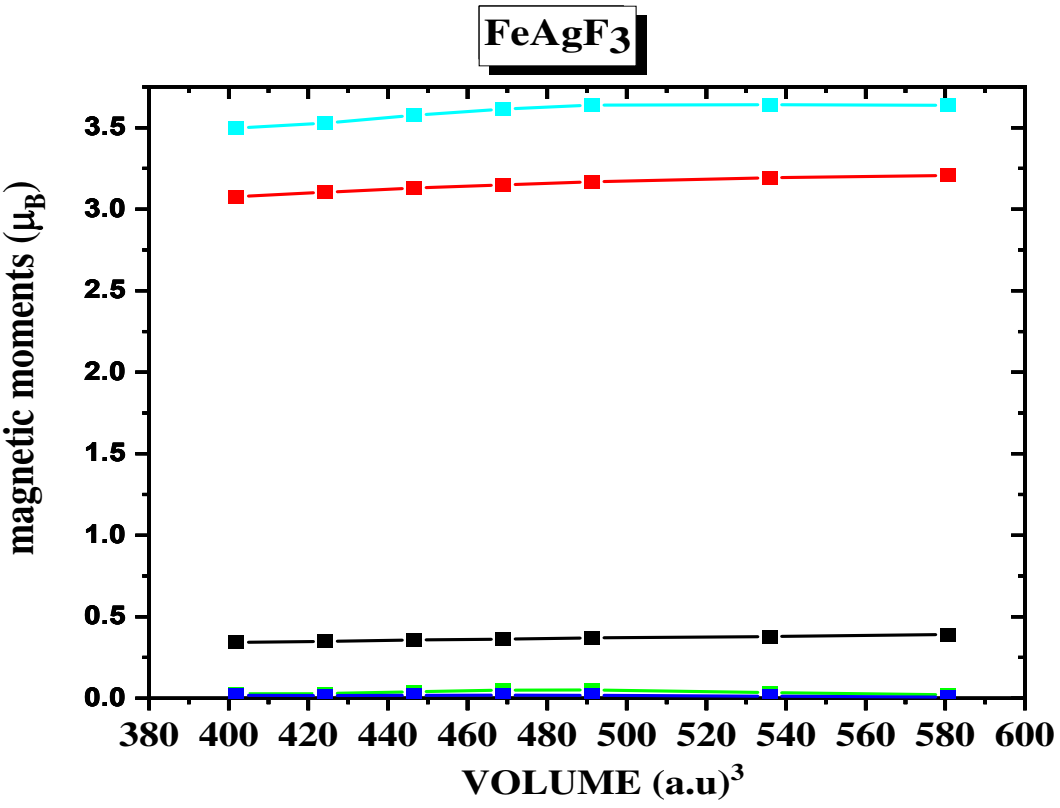

Figure II.8: Changes in the total and molecular magnetic moments of the compound **$FeAgF_3$** as a function of changes in the unit cell volume using the **GGA** approximation.

Figure(II.7) shows that the compound **$CoAgF_3$** has a rather large magnetic moment of 3.2(μ_b) It can also be realized that the atomic magnetic moments of the atoms **Ag** - **F** - **Co** have positive values, and therefore the magnetic moments of the three atoms are directed to each other in a parallel manner (in the same direction), and from this the compound has a farromagnetic nature **(FM)**, which was previously confirmed when studying the structural properties of this compound. It is also noted that the two atoms, **Ag** and **F**, have an almost non-existent magnetic moment, while the cobalt atom, **Co**, has the dominant contribution to this total moment.

As for the effect of the side length of the crystal cell on the magnetic moment of the compound, we note that no matter how long the side length of the crystal cell increases, the total magnetic moment remains constant.

Figure (II.8) shows that the FeAgF3 compound has a greater magnetic moment of 3.5(μ_b). It can also be realized that the atomic magnetic moments of the Ag - F - Fe atoms have positive values, and thus the magnetic moment as the three atoms are oriented towards each other in parallel. (In the same direction), including that the compound has a ferromagnetic nature (FM), which was previously confirmed when studying the structural properties of this compound. It is also noted that the Ag and F atoms have an almost non-existent magnetic moment, while the Fe atom has the dominant contribution to this total moment.

As for the effect of the side length of the crystal cell on the magnetic moment of the compound, we notice that the total magnetic moment is slightly affected by the change in volume.

5- Electronic properties:

The investigation of electronic properties is crucial, as it enables us to identify and select the most suitable electric or electronic fields for utilizing a given material. This goal is accomplished by thoroughly examining the electronic characteristics of the compound in question. Consequently, we analyzed the energy ranges of various compounds to ascertain their electronic behavior, classifying them as insulators, conductors, or semiconductors. Additionally, we evaluated the density of states to pinpoint the atomic orbitals that significantly impact each energy range. This understanding helps us comprehend the formation of interatomic bonds within the material..

5-1- Band structure

In solid systems with a periodic structure, electrons initially occupy distinct energy levels. The periodic potential created by the regular arrangement of atoms in a crystal lattice causes the electrons to interact with each other. As a result of these interactions, the individual energy levels of isolated atoms hybridize and split into multiple closely spaced levels. This process creates a continuous range of energy levels, known as an energy band, or energy spectrum. Understanding the formation of these energy bands is crucial for determining the electronic properties of materials, which dictates whether a material acts as an insulator, conductor, or semiconductor [23]. Each energy band differs from others in the region it occupies (the conduction or valence region), as well as the width of the band, especially the electrons in the atomic orbitals that contribute to its creation.

The energy bands of both compounds **$CoAgF_3$** and **$FeAgF_3$** were studied in the most stable state in the first Brillouin region defined in the inverse lattice space at points with high symmetry, following the path **(R-Γ-X-M-Γ)**, where the coordinates of these points are given for both compounds **$CoAgF_3$** and **$FeAgF_3$**. In the following **figure (II.9):**

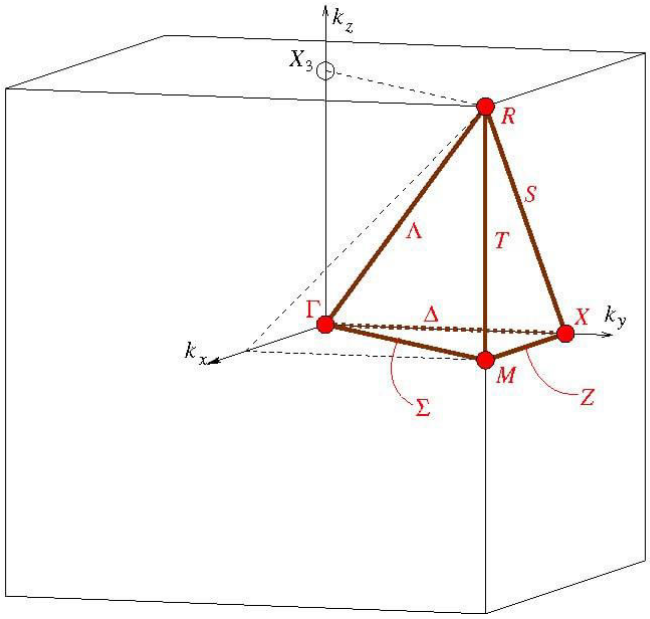

Figure (II.9): The first Brillouin zone and the highly symmetry points used in calculating the energy bands for **$CoAgF_3$** and **$FeAgF_3$**

5-2- Total (TDOS) and partial (PDOS) density of states

Based on the distribution curves of the energy density of macro and partial states, it is easy to determine which electrons are responsible for the production of each energy band and to explain the formation of particular atomic bonds. The number of electronic states that can exist at a given energy in a crystal system is determined by its density of state (TDOS). In addition to understanding which atomic orbitals form bonds and what kind of hybridization takes place, state density can be used as a supplementary tool to explain the creation of specific energy bands.

The density of state is defined for energies confined in a field $[\varepsilon, \varepsilon + \delta\varepsilon]$ So that it represents $g(\varepsilon)d\varepsilon$ The number of energy states present in this field per unit volume [23], as the total state density is the sum of all possible states that have energies confined to the energy field **[ε,ε+δε].**

The state density expression is given by its relationship to the band structure according to the following mathematical formula:

$$g(\varepsilon) = \sum_i 2 \int \frac{dk}{(2\pi)^3} \delta\left(\varepsilon - \varepsilon_{i,k}\right) \ldots\ldots\ldots\ldots\ldots \text{(II. 4)}$$

We can rewrite the overall density of state with the equation:

$$g(\varepsilon) = \frac{1}{\Omega} \sum_i 2 \sum_k \langle \varphi_{i,k} | \varphi_{i,k} \rangle \, \delta\left(\varepsilon - \varepsilon_{i,k}\right) \ldots\ldots\ldots\ldots\ldots \text{(II. 5)}$$

Where **Ω** represents the volume of the solid body and $|\varphi_{i,k}\rangle$ They are the special cases of solutions of the **Cohen-Sham** equation corresponding to the special values $\varepsilon_{i,k}$

We can calculate the partial density $n_i\ (\varepsilon)$ of states (PDOS) after projecting the total density of state (TDOS) onto the orbitals to obtain the partial contribution of each atomic orbital as indicated in reference [40]:

$$n_i\ (\varepsilon) = \sum_n \delta\ (\varepsilon - \varepsilon_n) |P_{ni}^a|^2 \ \ldots\ldots\ldots\ldots \text{(II. 6)}$$

5-3- Analysis of the structure curves of the energy bands and the density of total and paartial density of states of CoAgF3:

According to **Figure (II-10)**, we studied the curve of the energy bands in both spin states of the compound **$CoAgF_3$** as follows:

In both the up and down spin cases, the band structure curves led to an overlap between the conduction bands and the valence bands, which confirms the metallic behavior of this compound.

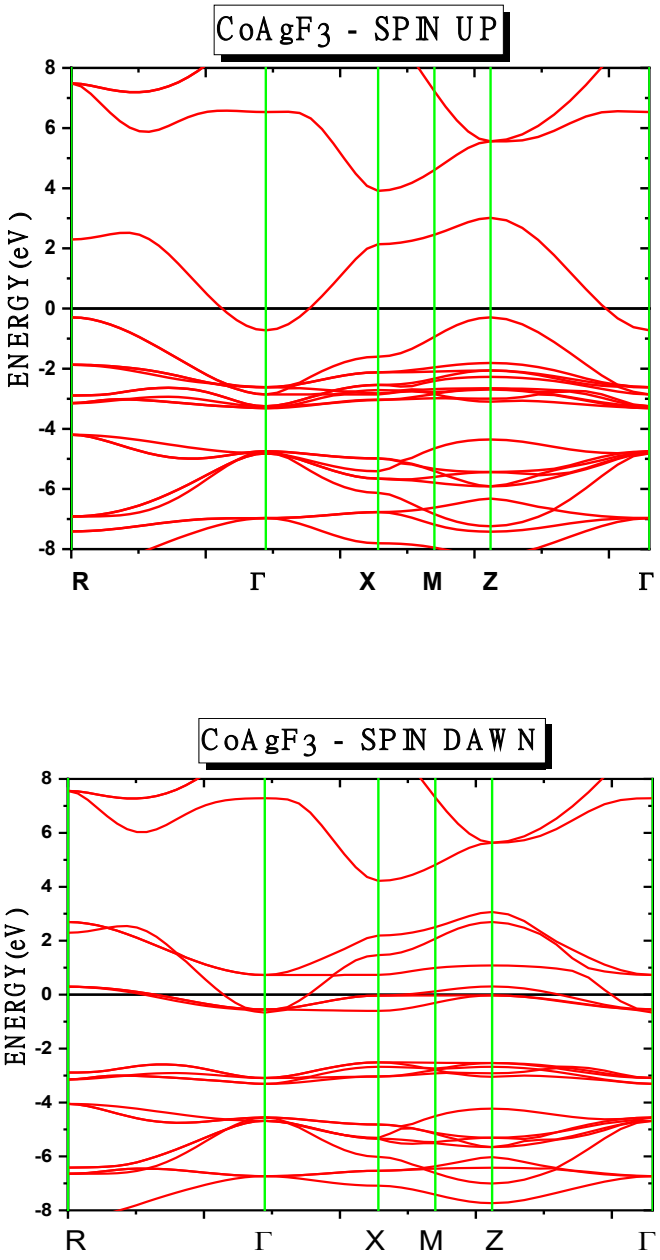

Figure (II.10): Structure curve of the energy bands of $CoAgF_3$ in both spin states calculated using the **mBJ** approximation.

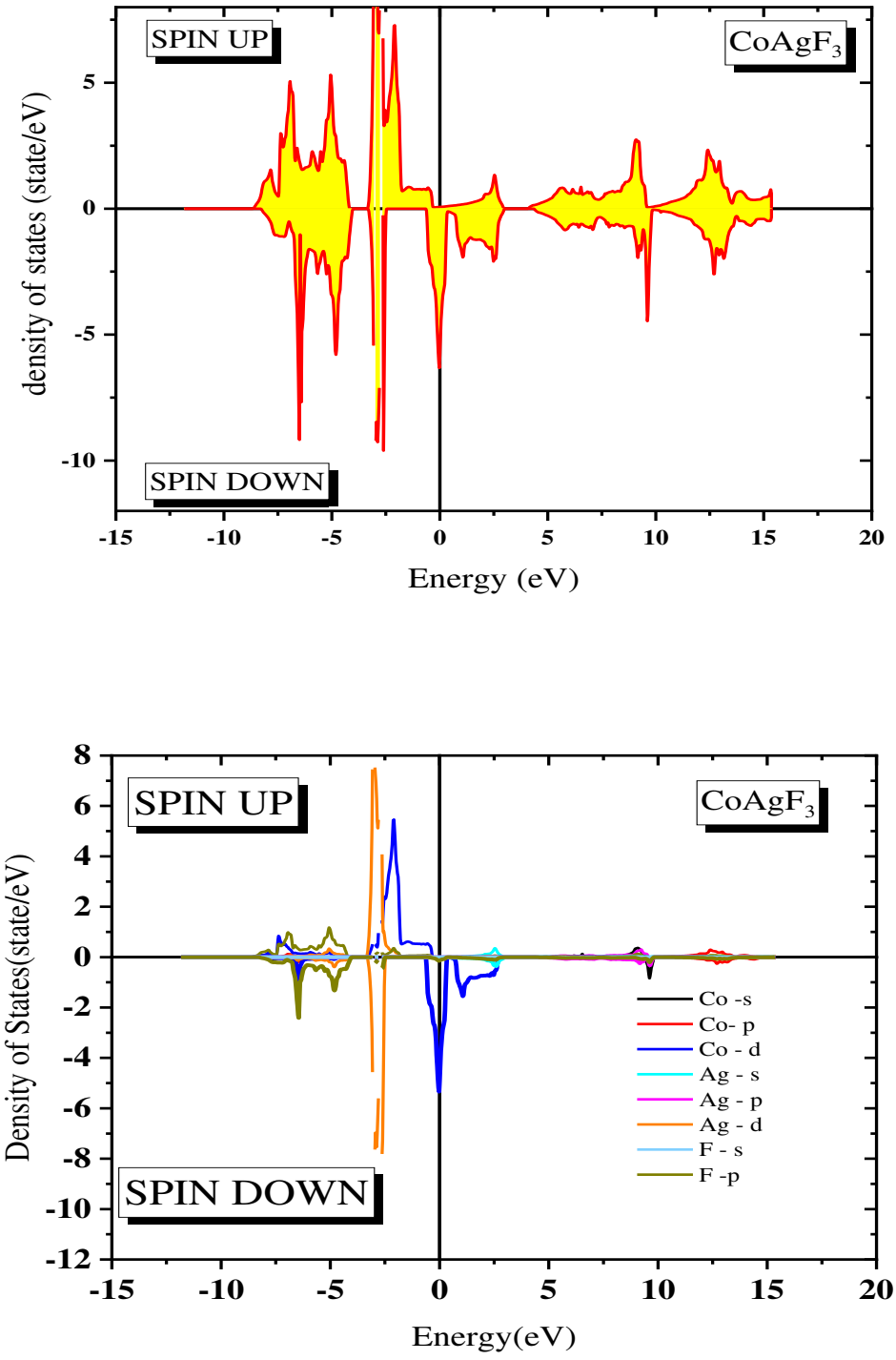

Figure (II.11): Distribution of the density of total and partial states of the compound **$CoAgF_3$** calculated using the **mBJ** approximation in the case of (**spin down**) and(**spin up**).

Figure (II.11) shows the distribution of both the total and partial state densities of the compound **$CoAgF_3$** calculated using the **mBJ** approximation in the case of **(spin down)** and **(spin up)**, through which we can record the following observations:

Spin-Up State

We observed a density of states at the Fermi level, indicating that this compound exhibits conductive behavior in the spin-up state. Additionally, several scattered energy peaks were noted, allowing us to distinguish three significant regions:

First Region [-7.5 eV, -4 eV]: This region shows a contribution from the d-orbital electrons of the Co atom and a weak contribution from the p-orbital electrons of the F atom.

Second Region [-4 eV, Fermi Level]: Here, we see contributions from the d-orbital electrons of both the Ag and Co atoms.

Spin-Down State

In the spin-down state, the compound demonstrates metallic behavior, as evidenced by the presence of a density of states at the Fermi level. The overall density of states distribution is spread across four key regions:

First Region [-7.5 eV, -4 eV]: Similar to the spin-up state, this region shows contributions from the d-orbital electrons of the Co atom and a minor contribution from the p-orbital electrons of the F atom.

Second Region [-4 eV, -3 eV]: This region features contributions from the d-orbital electrons of the Ag atom.

Third Region [-1 eV, 2 eV]: Here, we observe contributions from the

d-orbital electrons of the Ag atom.

3-4 Analysis of the energy bands curves and the total and molecular density of states of the compound FeAgF3:

According to **Figure (II 12)**, we noticed that the electronic behavior of the compound FeAgF3 does not differ from that of the compound CoAgF3, as it clearly appears that there is an absence of the energy gap and an overlap between the conduction and valence bands at the Fermi level.

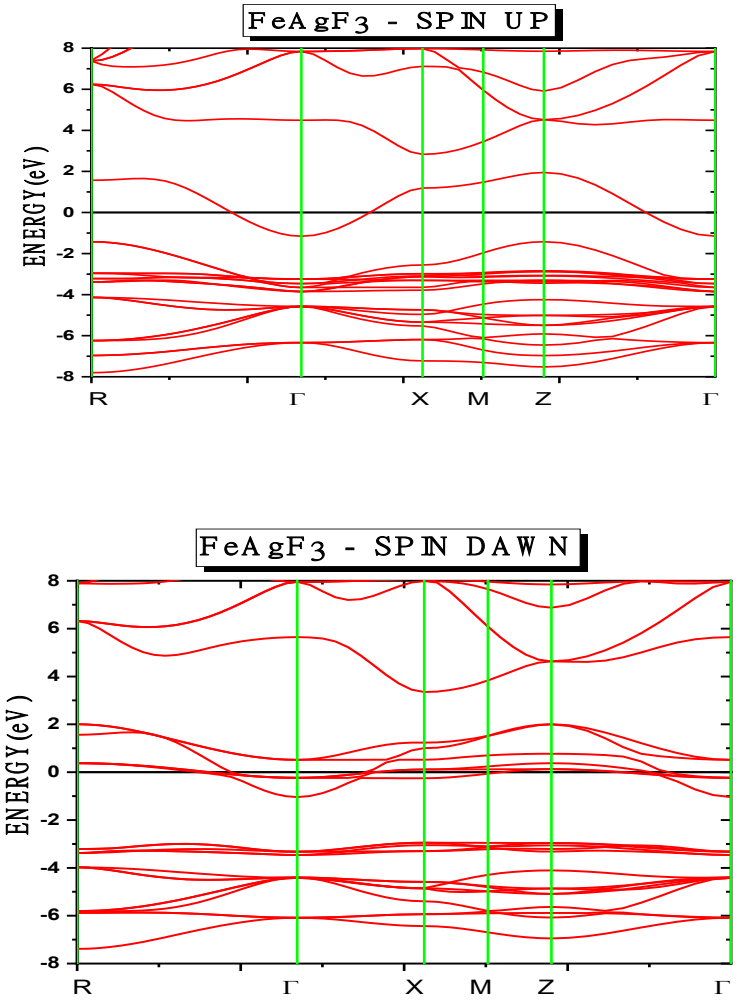

Figure (II.12): Structure curve of the energy bands for $FeAgF_3$ in both **spin** states calculated using the **mBJ** approximation.

To provide a better explanation of how these bands are formed, we resort to analyzing the density distribution curves of the partial and total states of the compound **$FeAgF_3$** in both spin states, as shown in **Figure (II 12).**

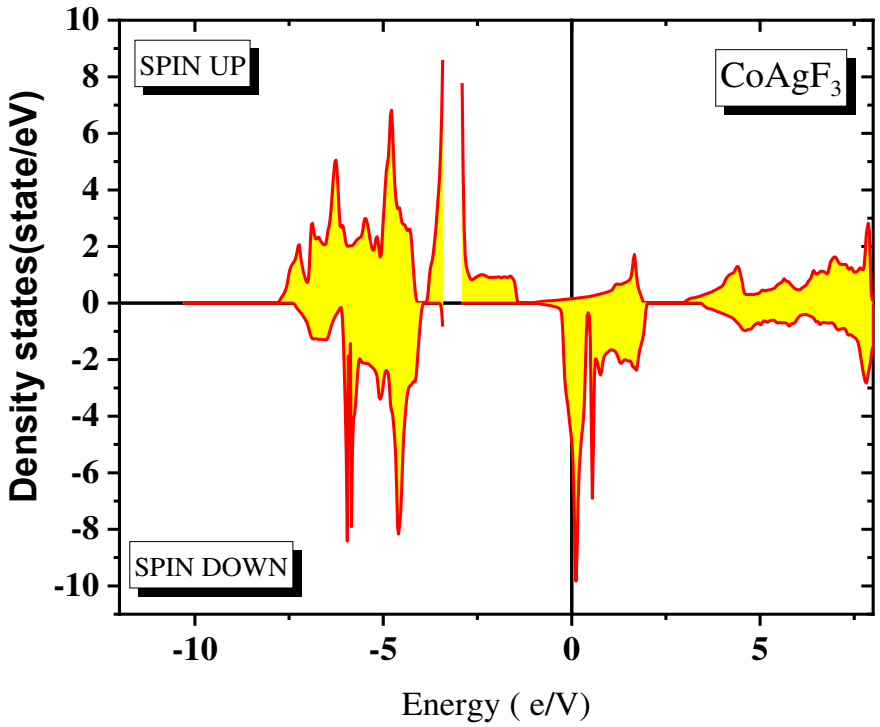

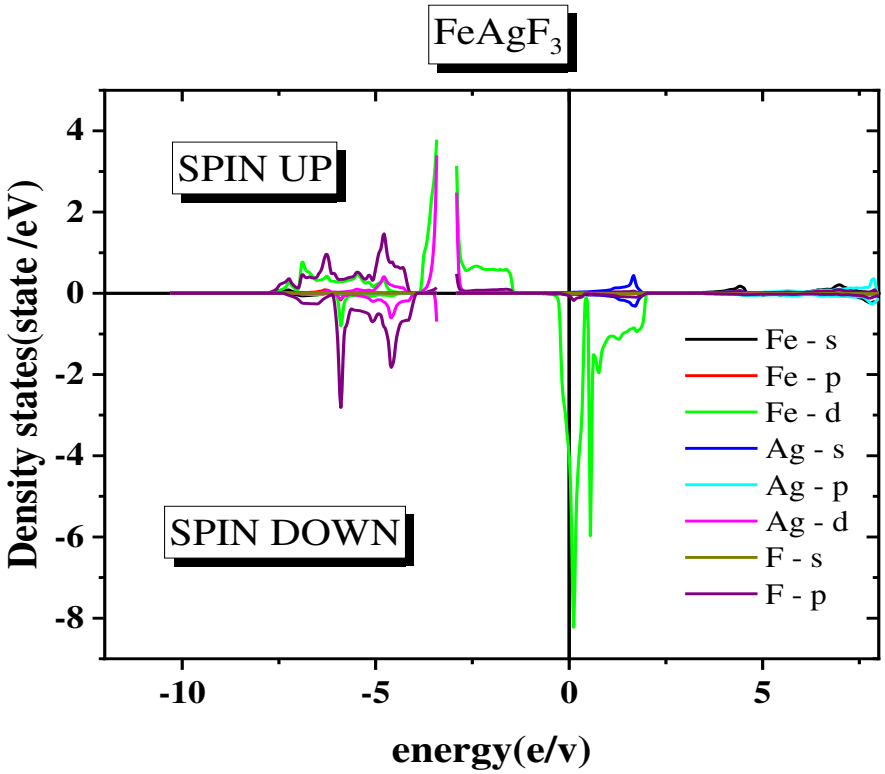

Figure (II.13): Distribution of the total and molecular density of states of **$FeAgF_3$** calculated using the **mBJ** approximation in the case of (spin down) and (spin up).

Figure (II.13) shows the distribution of both the total and partial state densities of the compound **$FeAgF_3$** calculated using the **mBJ** approximation in the case of (spin down) and(spin up) , Based on our observations, we can summarize the findings as follows:

Spin-Up State

We observed a density of states at the Fermi level, confirming that this compound exhibits conductive behavior in the spin-up state. Additionally, several scattered energy peaks were identified, allowing us to distinguish three significant regions:

First Region [-7.5 eV, -4 eV]: Contributions from the

d-orbital electrons of the Ag atom and the

p-orbital electrons of the F atom were noted.

Second Region [-4 eV, Fermi Level]: This region shows contributions from the

d-orbital electrons of the Fe atom and a weaker contribution from the

d-orbital electrons of the Ag atom.

Third Region [2 eV, 3 eV]: Here, we observe contributions from the

s-orbital electrons of the Ag atom.

Spin-Down State

The distribution spectrum of the overall density of states in the spin-down state is divided into four key regions:

First Region [-7.5 eV, -4 eV]: Contributions from the

d-orbital electrons of both the Ag and Fe atoms, along with contributions from the

p-orbital electrons of the F atom, were observed.

Second Region [-0.5 eV, 3 eV]: A strong contribution from the

d-orbital electrons of the Fe atom was noted.

References

[1] J.C. Slater, Damped electron waves in crystals, Phys. Rev. 51 (1937) 840.

[2] D.D. Koelling, G.O. Arbman, Use of energy derivative of the radial solution in an augmented plane wave method: application to copper, J. Phys. F Met. Phys. 5 (1975) 2041.

[3] O.K. Andersen, Linear methods in band theory, Phys. Rev. B. 12 (1975) 3060.

[4] D.R. Hamann, Semiconductor charge densities with hard-core and soft-core pseudopotentials, Phys. Rev. Lett. 42 (1979) 662.

[5] D. Singh, H. Krakauer, H-point phonon in molybdenum: Superlinearized augmented-plane-wave calculations, Phys. Rev. B. 43 (1991) 1441.

[6] E. Sjöstedt, L. Nordström, D.J. Singh, An alternative way of linearizing the augmented plane-wave method, Solid State Commun. 114 (2000) 15–20.

[7] P. Blaha, K. Schwarz, G. Madsen, D. Kvasnicka, J. Luitz, Wien2k, (2001).

[8] W. Kohn, L.J. Sham, Self-Consistent Equations Including Exchange and Correlation Effects, Phys. Rev. 140 (1965) A1133–A1138. https://doi.org/10.1103/physrev.140.a1133.

[9] J.P. Perdew, K. Burke, M. Ernzerhof, Generalized Gradient Approximation Made Simple, Phys. Rev. Lett. 77 (1996) 3865–3868. https://doi.org/10.1103/physrevlett.77.3865.

[10] A.D. Becke, E.R. Johnson, A simple effective potential for exchange, J. Chem. Phys. 124 (2006) 221101.

[11] O.K. Andersen, T. Saha-Dasgupta, Muffin-tin orbitals of arbitrary order, Phys. Rev. B. 62 (2000) R16219.

[12] F. Izumi, K. Momma, Three-dimensional visualization in powder diffraction, in: Solid State Phenom., Trans Tech Publ, 2007: pp. 15–20.

[13] K. Momma, F. Izumi, VESTA 3 for three-dimensional visualization of crystal, volumetric and morphology data, J. Appl. Crystallogr. 44 (2011) 1272–1276.

[14] K. Momma, F. Izumi, VESTA: a three-dimensional visualization system for electronic and structural analysis, J. Appl. Crystallogr. 41 (2008) 653–658.

[15] K. Momma, F. Izumi, An integrated three-dimensional visualization system VESTA using wxWidgets, Comm. Crystallogr Comput IUCr Newslett. 7 (2006) 106–119.

[16] F.D. Murnaghan, The compressibility of media under extreme pressures, Proc. Natl. Acad. Sci. U. S. A. 30 (1944) 244.

[17] L.Q. Jiang, J.K. Guo, H.B. Liu, M. Zhu, X. Zhou, P. Wu, C.H. Li, Prediction of lattice constant in cubic perovskites, J. Phys. Chem. Solids. 67 (2006) 1531–1536.

[18] A.S. Verma, V.K. Jindal, Lattice constant of cubic perovskites, J. Alloys Compd. 485 (2009) 514–518.

[19] S.S. Essaoud, Z. Charifi, H. Baaziz, G. Uğur, Ş. Uğur, Electronic structure and magnetic properties of manganese-based MnAs1- xPx ternary alloys, J. Magn. Magn. Mater. 469 (2019) 329–341.

[20] S. Saad Essaoud, Les composés à base de manganèse: investigation théorique des propriétés structurales électroniques et magnétiques, DOCTORAT THESIS, 2020. https://doi.org/10.13140/RG.2.2.30742.68169.

[21] S.S. Essaoud, A.S. Jbara, First-principles calculation of magnetic, structural, dynamic, electronic, elastic, thermodynamic and thermoelectric properties of Co2ZrZ (Z= Al, Si) Heusler alloys, J. Magn. Magn. Mater. (2021) 167984.

[22] O. Volnianska, P. Boguslawski, Magnetism of solids resulting from spin polarization of p orbitals, J. Phys. Condens. Matter. 22 (2010) 073202. https://doi.org/10.1088/0953-8984/22/7/073202.

[23] J.M.D. Coey, ed., Magnetism of localized electrons on the atom, in: Magn. Magn. Mater., Cambridge University Press, Cambridge, 2010: pp. 97–127. https://doi.org/10.1017/CBO9780511845000.005.

[24] M.D. Johannes, I.I. Mazin, Microscopic origin of magnetism and magnetic interactions in ferropnictides, Phys. Rev. B. 79 (2009) 220510.

[25] M. Valant, T. Kolodiazhnyi, I. Arčon, F. Aguesse, A.-K. Axelsson, N.M. Alford, The Origin of Magnetism in Mn-Doped SrTiO3, Adv. Funct. Mater. 22 (2012) 2114–2122.

[26] J. Degauque, Magnétisme et matériaux magnétiques: introduction, J. Phys. IV. 2 (1992) C3-1.

[27] P. Langevin, Sur la théorie du magnétisme, J Phys Theor Appl. 4 (1905) 678–693.

[28] I. Jum'h, H. Baaziz, Z. Charifi, A. Telfah, Electronic and Magnetic Structure and Elastic and Thermal Properties of Mn 2-Based Full Heusler Alloys, J. Supercond. Nov. Magn. (n.d.) 1–12.

CONCLUSION

Conclusion

The explore of the structural, magnetic, and electronic properties of perovskite compounds $CoAgF_3$ and $FeAgF_3$ was conducted using density functional theory (DFT), with the Generalized Gradient Approximation (GGA) used for structural and magnetic properties and the modified Becke-Johnson (mBJ) approximation for electronic properties. The Wien2k program was employed to solve the Schrödinger equation for multiple crystal systems, using the simplified Kohn-Sham equations. Both compounds were found to have a simple cubic structure with five atoms, facilitating quick calculations, and $CoAgF_3$ was observed to have a smaller cell volume compared to $FeAgF_3$. The mechanical analysis showed that both compounds have a large compressibility coefficient, indicating high resistance to deformation, with $CoAgF_3$ having a higher bulk modulus than $FeAgF_3$. In terms of magnetic properties, both compounds are magnetically stable and exhibit ferromagnetic properties. $CoAgF_3$'s high magnetic moment is primarily due to Cobalt (Co) atoms and remains stable regardless of cell size changes, whereas $FeAgF_3$'s high magnetic moment is mainly due to Iron (Fe) atoms and shows slight sensitivity to cell size changes. Additionally, in their most stable states, both compounds demonstrate vector behavior, confirmed through GGA calculations. The electronic properties reveal that electrons from Co-d, Ag-d, F-p, and Fe-d orbitals significantly contribute to the formation of energy bands and atomic bonds. This comprehensive study highlights the potential applications of $CoAgF_3$ and $FeAgF_3$ in fields requiring materials with high magnetic moments and strong resistance to compression.

ملخص

فـي عملنـا هـذا قمنـا بدراسـة نظريـة لحسـاب الخـواص البنيويـة ، المغناطيسـية و الالكترونيـة للمركبين $CoAgF_3$ و$FeAgF_3$ وذلك باستعمال طريقة الأمواج المستوية المتزايدة خطيا (FP-LAPW) المعتمدة على نظرية دالية الكثافة (DFT) ، لحساب الكمون (تبادل – ارتباط) استعملنا تقريب التدرج المعمم (*GGA*) في دراسة خواص المركبين ، في حساب الخواص البنيوية قمنا بحساب ثابت الشبكة ، معامل الانظغاطية ، ولفهم السلوك الالكتروني لكلا المركبين قمنا بتحليل بنية عصابات الطاقة الإلكترونية وأطياف الكثافة الحالات الإلكترونية (DOS) الكلية و الجزئية (PDOS)،

و في النهاية قمنا بحساب العزم المغناطيسي الكلي و الجزئي للذرات المكونة للمركبين كما قمنا بدراسة تأثير الضغط على تغيرات العزم المغناطيسي الكلي للخلية البلورية.

Abstract

In this work, we conducted a theoretical study to calculate the structural, magnetic and electronic properties of the compounds $CoAgF_3$ and $FeAgF_3$ using the linearly increasing plane wave method.

(FP-LAPW) based on density function theory (DFT), to calculate potential (exchange - correlation)

We used the generalized gradient approximation (GGA) to study the properties of the two compounds. In calculating the structural properties, we calculated the lattice constant and the compressibility coefficient. To understand the electronic behavior of both compounds, we analyzed the structure of the electronic energy bands and the overall density spectra of the electronic states (DOS).

and partial (PDOS),

In the end, we calculated the total and partial magnetic moments of the atoms that make up the two compounds as we did

By studying the effect of pressure on changes in the total magnetic moment of the crystal cell.